Challenges and Progress in Computational Materials Science

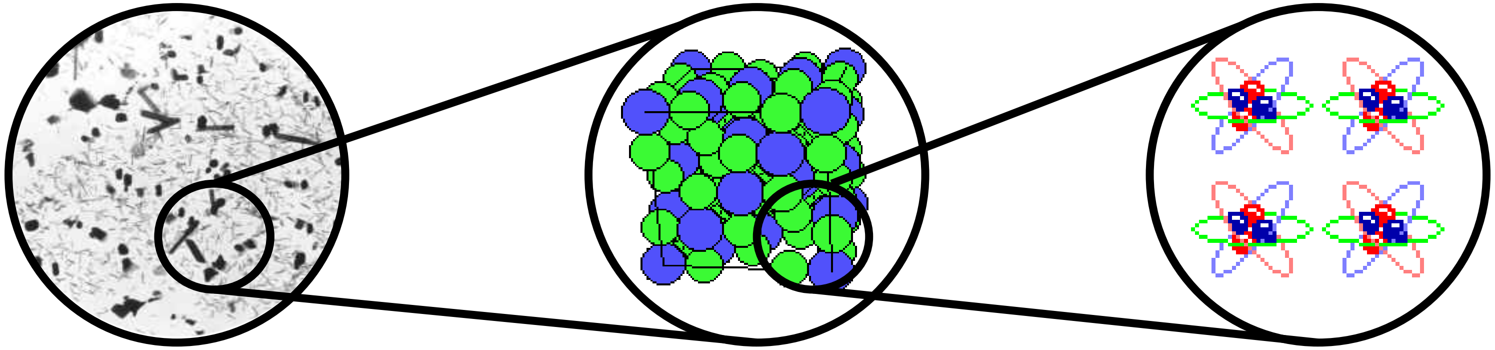

P. A. Korzhavyi
Applied Materials Physics
Department of Materials Science and Engineering
School of Industrial Engineering and Management
Royal Institute of Technology (KTH), Stockholm

Computational Physics (CP)

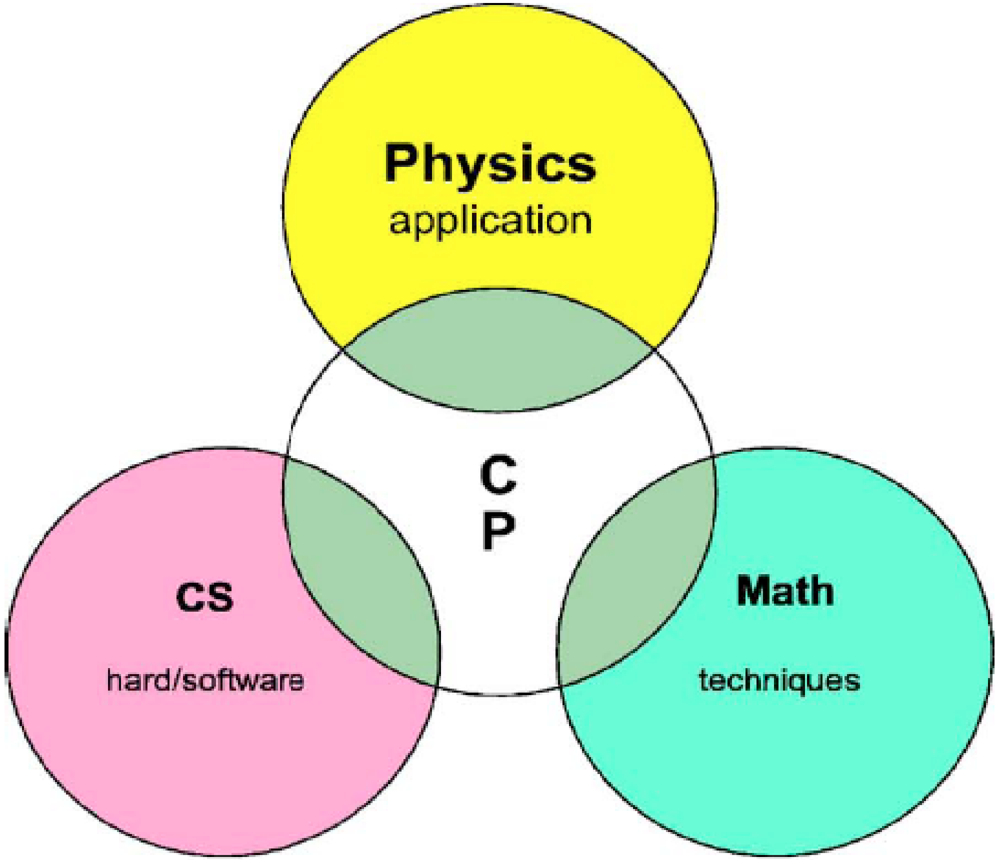

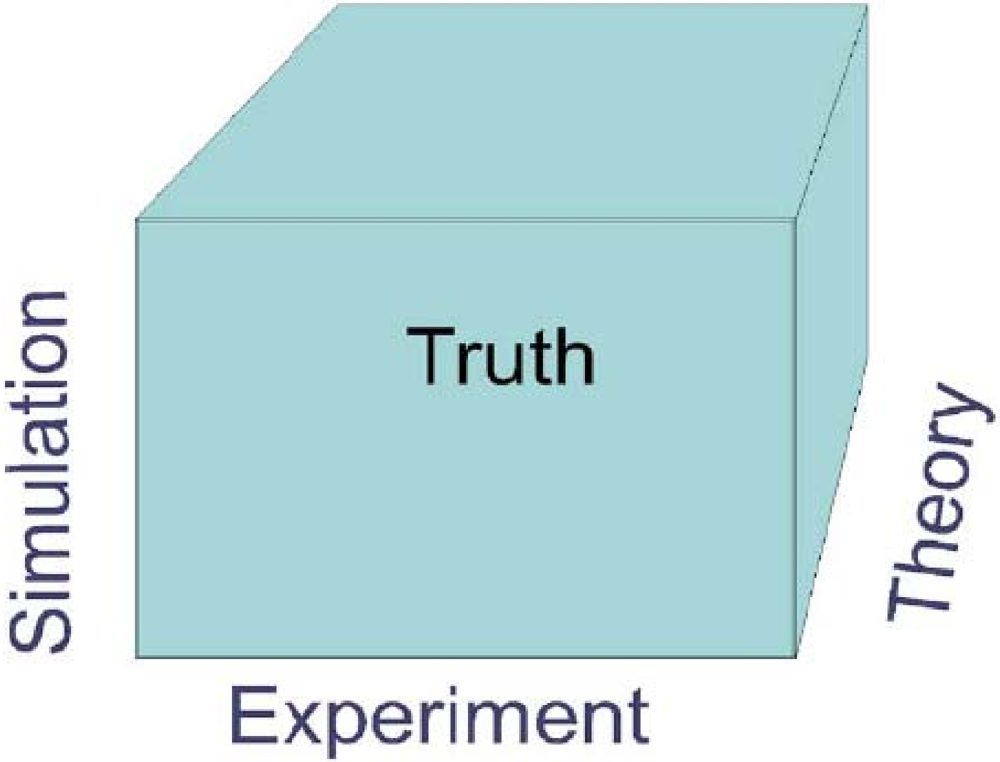

Source: R. H. Landau, Resource Letter CP-2: Computational Physics, *American Journal of Physics* **76**, 296 (2008).

Challenges for Materials Science

- Construction materials for the new-generation **energy** production plants and engines:
  - New (higher temperature) coal-burning plants;
  - Generation-IV (fast neutron) nuclear reactors;
  - Thermo-nuclear reactors;
  - Wave, wind, solar, *etc.* power stations.

  (lifetime ~ 10-50 years)
- Materials for **safe** immobilization and disposal of nuclear waste (industrial & military): (lifetime ~ 100 000 years)

Challenge: Generation-IV nuclear power reactors (breeders)

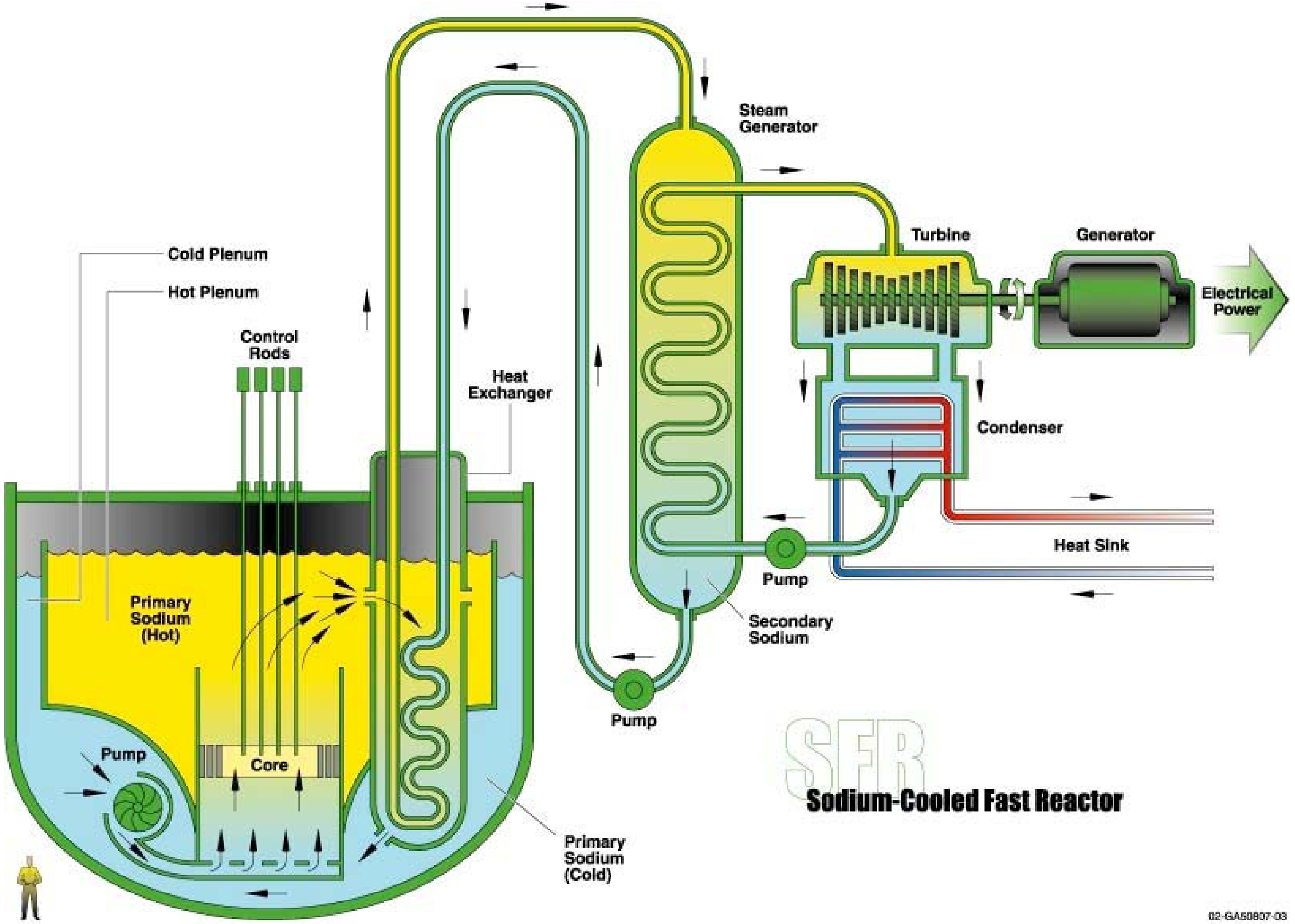

The economical feasibility of Gen-IV reactors is directly related to the lifetime of structural materials.

Desired materials lifetime ~ 30 - 50 y.

Challenge: Safe disposal of nuclear waste

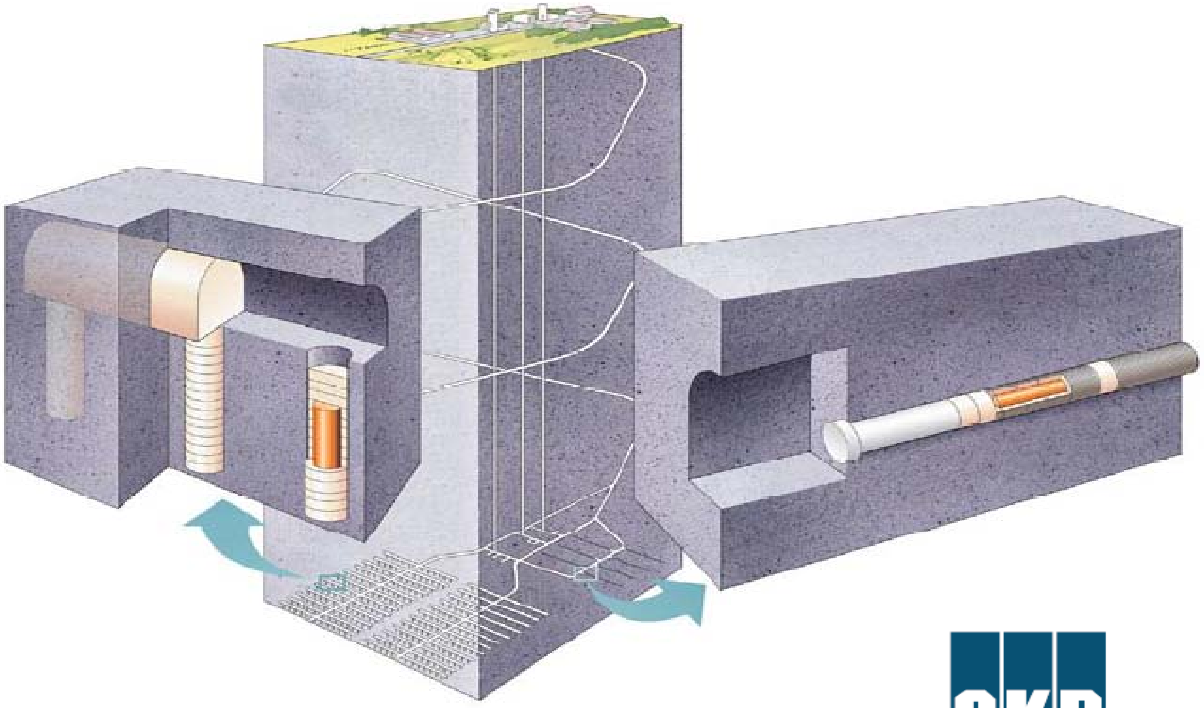

Svensk Kärnbränslehantering AB
Swedish Nuclear Fuel and Waste Management Co
Box 5864, SE-102 40 Stockholm, Sweden
Telephone +46 8 459 84 00 Fax +46 8 661 57 19
www.skb.se info@skb.se

Reliable predictions of materials' behaviour (spent UO$_2$ fuel, iron insert, and copper canister) should be made for the whole period of storage.

Storage period about 300 000 y.

Challenges for Materials Science

- Materials engineers need **novel design approaches**: the new materials should be developed during a relatively short period (as compared to the materials’ lifetime).
- Normal experimental testing of materials (during 1/3 of the expected lifetime) is not affordable.
- We have to rely on our understanding of materials as well as on computer models.
- Fundamental understanding and accurate models of materials are needed.

Impact of XXth century physics on Materials Science

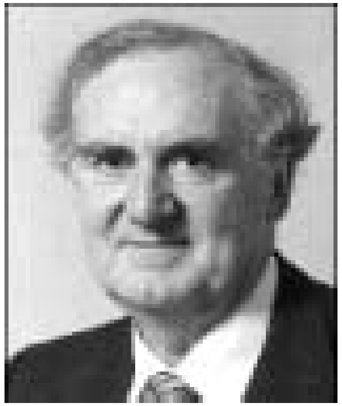

Sir Alan Cottrell

> *It was the century when we understood materials, scientifically, for the first time-what they are and how they perform. Two advances have been outstanding in making this possible:* ***X-ray analysis****, which showed us where the atoms are inside materials; and* ***quantum mechanics****, which explained how they interact and produce the bulk properties of matter.*

Alan Cottrell

Centennial Report [MRS Bulletin **25**, 43 (2000)]

Computational experiments on ”virtual” matter

INPUT

SOFTWARE

OUTPUT

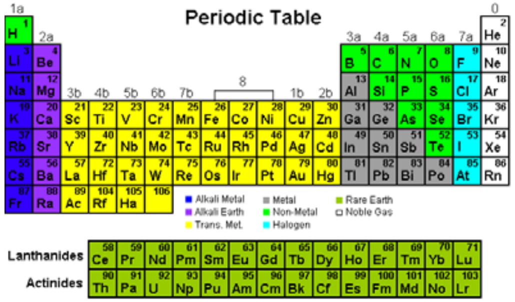

Periodic Table

1a	2a	3b	4b	5b	6b	7b	8			1b	2b	3a	4a	5a	6a	7a	0
1 H																	2 He
3 Li	4 Be											5 B	6 C	7 N	8 O	9 F	10 Ne
11 Na	12 Mg											13 Al	14 Si	15 P	16 S	17 Cl	18 Ar
19 K	20 Ca	21 Sc	22 Ti	23 V	24 Cr	25 Mn	26 Fe	27 Co	28 Ni	29 Cu	30 Zn	31 Ga	32 Ge	33 As	34 Se	35 Br	36 Kr
37 Rb	38 Sr	39 Y	40 Zr	41 Nb	42 Mo	43 Tc	44 Ru	45 Rh	46 Pd	47 Ag	48 Cd	49 In	50 Sn	51 Sb	52 Te	53 I	54 Xe
55 Cs	56 Ba	57 La	72 Hf	73 Ta	74 W	75 Re	76 Os	77 Ir	78 Pt	79 Au	80 Hg	81 Tl	82 Pb	83 Bi	84 Po	85 At	86 Rn
87 Fr	88 Ra	89 Ac	104 Rf	105 Ha	106												

■ Alkali Metal ■ Alkali Earth ■ Trans. Met. ■ Metal ■ Non-Metal ■ Halogen ■ Rare Earth □ Noble Gas

Lanthanides	58 Ce	59 Pr	60 Nd	61 Pm	62 Sm	63 Eu	64 Gd	65 Tb	66 Dy	67 Ho	68 Er	69 Tm	70 Yb	71 Lu
Actinides	90 Th	91 Pa	92 U	93 Np	94 Pu	95 Am	96 Cm	97 Bk	98 Cf	99 Es	100 Fm	101 Md	102 No	103 Lr

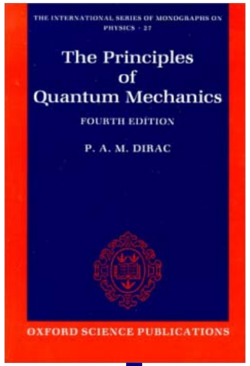

THE INTERNATIONAL SERIES OF MONOGRAPHS ON PHYSICS · 27

The Principles
of
Quantum Mechanics

FOURTH EDITION

P. A. M. DIRAC

OXFORD SCIENCE PUBLICATIONS

Physical laws
Universal constants
Methods
Approximations

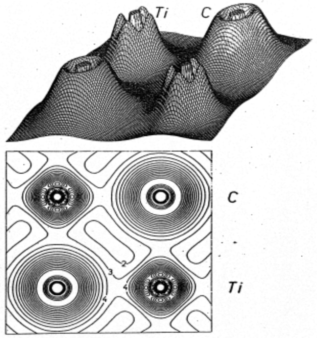

FIG. 1. Theoretical (static) valence-electron density of TiC in the (100) plane obtained by LAPW calculations (Ref. 18). Contour intervals, $0.1e$ Å^{-3}, cutoff at $1.7e$ Å^{-3}.

Atomic numbers & coordinates.

HARDWARE

1. Electron density
2. Total energy

Derivatives: forces, properties, *etc.*

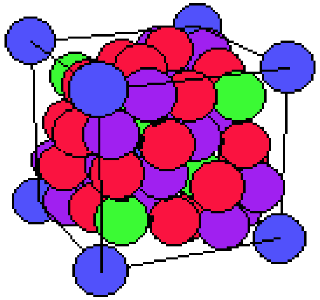

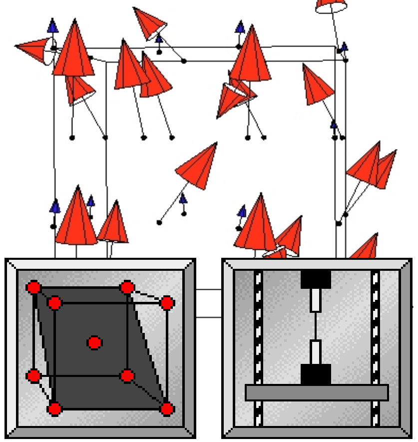

HERO-M: Hierarchic Engineering of Industrial Materials

J. Ågren

B. Johansson

FEM
CAD-CAM

Engineering design

Thermo-Calc
DICTRA
Phase Field
Life time assessment
Many years

Continuum models

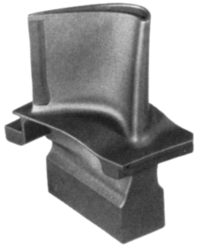

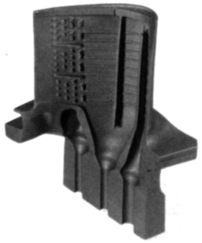

Phenomenological models
- Macro simulation
- Micro structure

Kinetic Monte Carlo
>1 million atoms,
20 nm, long times

Atomic level simulation
- Statistical mechanics
- Classical dynamics
- Force field

Molecular dynamics
100000 ca 10 nm 10^{-6} s

Memika

Density functional theory:
ca 100 atoms
1 nm, 0 K

Fundamental models
- Quantum mechanics
- Quantum theory

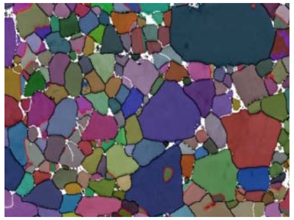

Size 1 (Å) 10 (Å) 100 (Å) 1 (μm) 1 (mm)

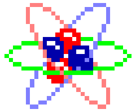

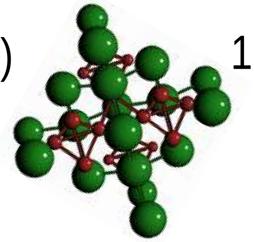

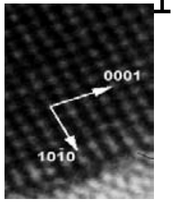

Schrödinger equation

$$\hat{H}\Psi(\mathbf{r},\mathbf{R}) = \left[\hat{H}_{\mathbf{r}} + \hat{H}_{\mathbf{R}} + \hat{H}_{\mathbf{r},\mathbf{R}}\right]\Psi(\mathbf{r},\mathbf{R}) = E\Psi(\mathbf{r},\mathbf{R})$$

Depends on the coordinates of <u>all</u> the electrons ($\mathbf{r}_i$) <u>and</u> nuclei ($\mathbf{R}_I$) in the system:

$$\Psi(\mathbf{r},\mathbf{R}) \equiv \Psi(\mathbf{r}_1,\mathbf{r}_2,\mathbf{r}_3,\ldots,\mathbf{R}_1,\mathbf{R}_2,\mathbf{R}_3,\ldots) = \underbrace{\psi(\mathbf{r}_1,\mathbf{r}_2,\mathbf{r}_3,\ldots)}_{\text{electron wavefunction}} \cdot \underbrace{\varphi(\mathbf{R}_1,\mathbf{R}_2,\mathbf{R}_3,\ldots)}_{\text{wavefunction of nuclei}} \equiv \psi(\mathbf{r})\cdot\varphi(\mathbf{R})$$

$$\hat{H}_{\mathbf{r}} = [\underbrace{-\sum_i \nabla_i^2}_{\text{el. kin. energy}} + \underbrace{\frac{1}{2}\sum_{i\neq j}\frac{1}{|\mathbf{r}_i - \mathbf{r}_j|}}_{\text{el.-el. interaction}}]; \quad \hat{H}_{\mathbf{R}} = [\underbrace{-\sum_I \nabla_I^2}_{\text{nuc. kin. energy}} + \underbrace{\frac{1}{2}\sum_{I\neq J}\frac{Z_I Z_J}{|\mathbf{R}_I - \mathbf{R}_J|}}_{\text{nuc.-nuc. interaction}}]; \quad \hat{H}_{\mathbf{r},\mathbf{R}} = [\underbrace{-\sum_{i,J}\frac{Z_J}{|\mathbf{r}_i - \mathbf{R}_J|}}_{\text{el.-nuc. interaction}}]$$

For a solid with ~ 10^{24} charged particles the equation cannot be solved exactly!

<u>Adiabatic (Born-Oppenheimer) approximation</u> makes use of the fact that nuclei are much heavier (and, therefore, slower) than electrons. Therefore, electronic wave function can be determined first, while the nuclei are considered as static point-charges.

$$m_{\mathrm{p}} \approx 1840\cdot m$$

<u>Self-consistent field approach:</u> reduce the many body problem to a one-particle problem. Each electron moves in the effective potential created by the nuclei and *all the other* electrons. The problem is to be solved iteratively (*self-consistently*).

Density functional theory (DFT)


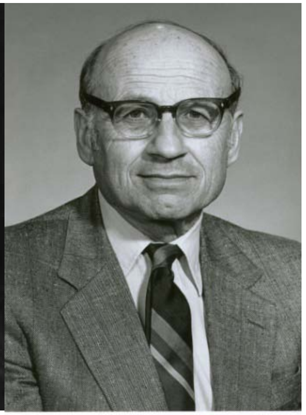

M. Born W. Kohn

Interpretation and use of the electron density

Total energy of the ground state is a unique functional

$$E = T_s[\rho] + \int d^3r\, \mathrm{v}_{ext}(\mathbf{r})\rho(\mathbf{r}) + \frac{1}{2}\int d^3r' \int d^3r \frac{\rho(\mathbf{r})\rho(\mathbf{r}')}{|\mathbf{r}-\mathbf{r}'|} + E_{xc}[\rho]$$

of electron density, $\rho(\mathbf{r}) = \sum_i^{occ} |\varphi_i(r)|^2$, where

$$T_s[\rho] = \sum_i^{occ} \int d^3r\, \varphi_i^*(\mathbf{r}) \left(-\frac{\nabla^2}{2}\right) \varphi_i(\mathbf{r})$$ is the kin. energy,

$\varphi_i(\mathbf{r})$ is a formal solution of Kohn-Sham equation:

$$\left(-\frac{\nabla^2}{2} + \mathrm{v}_{ext}(\mathbf{r}) + \int d^3r' \frac{\rho(\mathbf{r})}{|\mathbf{r}-\mathbf{r}'|} + \mathrm{v}_{xc}(\mathbf{r})\right)\varphi_i(\mathbf{r}) = \varepsilon_i \varphi_i(\mathbf{r})$$

where $$\mathrm{v}_{xc}(\mathbf{r}) = \frac{\delta E_{xc}[\rho]}{\delta\rho(\mathbf{r})}.$$

Note that $\varphi_i(\mathbf{r})$ is just an auxiliary function!

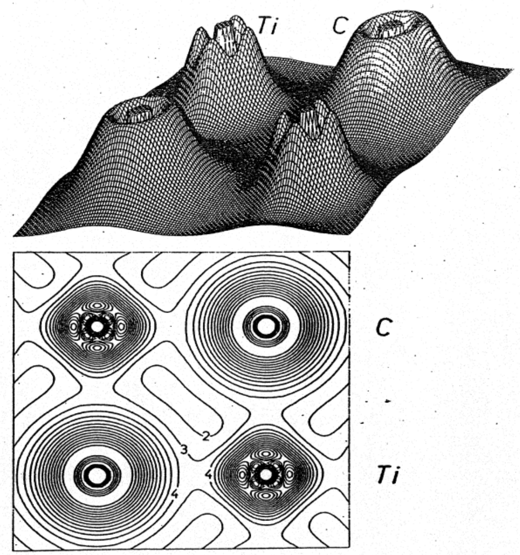

FIG. 1. Theoretical (static) valence-electron density of TiC in the (100) plane obtained by LAPW calculations (Ref. 18). Contour intervals, $0.1e$ Å^{-3}, cutoff at $1.7e$ Å^{-3}.

P. Blaha and K. Schwarz, (1983).

Exchange-correlation functionals E_{xc}

LDA*: $E_{xc}^{LDA} = \int d^3r\rho(\mathbf{r})\varepsilon_{xc}^{UEG}\left(\rho(\mathbf{r})\right)$, where $\varepsilon_{xc}^{UEG}(\rho)$ is the exchange-correlation energy per particle of a uniform electron gas (UEG) with density ρ. This quantity is known from quantum Monte Carlo calculations [D.M. Ceperley & B.J. Alder, *Phys. Rev. Lett*. **45**, 566 (1980)].

GGA*: $E_{xc}^{GGA} = \int d^3r\rho(\mathbf{r})\varepsilon_{xc}^{GGA}\left(\rho,\nabla\rho\right)$. Here $\varepsilon_{xc}^{GGA}\left(\rho,\nabla\rho\right)$ is not uniquely defined, many different forms have been proposed, e.g. **PBE** [J.P. Perdew, K. Burke, & M. Ernzerhof, *Phys. Rev. Lett*. **77**, 3865 (1996); *Ibid*. **78**, 1396 (1997)].

Meta-GGA: $E_{xc}^{MGGA} = \int d^3r\rho(\mathbf{r})\varepsilon_{xc}^{MGGA}\left(\rho,\nabla\rho,\nabla^2\rho,\tau\right)$, where $\tau = \frac{1}{2}\sum_i^{occ}\left|\nabla\varphi_i(r)\right|^2$ is the kinetic energy density. E.g., **PKZB** [J.P. Perdew, S. Kurth, A. Zupan, & P. Blaha, *Phys. Rev. Lett*. **82**, 5179 (1999)].

Hybride functionals, "exact exchange": $E_{xc}^{hyb}[\rho] = a\cdot\left(E_x - E_x^{GGA}\right) + E_{xc}^{GGA}$, where some fraction, a, of the exact exchange energy, E_x, is admixed to the GGA XC energy.

$$E_x = -\frac{1}{2}\sum_{i,j}^{occ}\int d^3r\int d^3r'\frac{\varphi_i^*(\mathbf{r})\varphi_j^*(\mathbf{r}')\varphi_i(\mathbf{r}')\varphi_j(\mathbf{r})}{\left|\mathbf{r}-\mathbf{r}'\right|}$$

* **LDA:** local density approximation; **GGA:** generalized gradient approximation

Popular software packages for electronic structure calculations

1. Vienna Ab-initio Simulation Package (VASP)
   http://cms.mpi.univie.ac.at/vasp/
2. Quantum ESPRESSO
   http://www.pwscf.org/
3. ABINIT http://www.abinit.org/
   http://www.abinit.org/about/presentation.pdf
4. SIESTA
   http://www.icmab.es/siesta/

Ab initio = from the beginning, from first principles

Input to *ab-initio* calculations

- Atomic numbers of the constituents

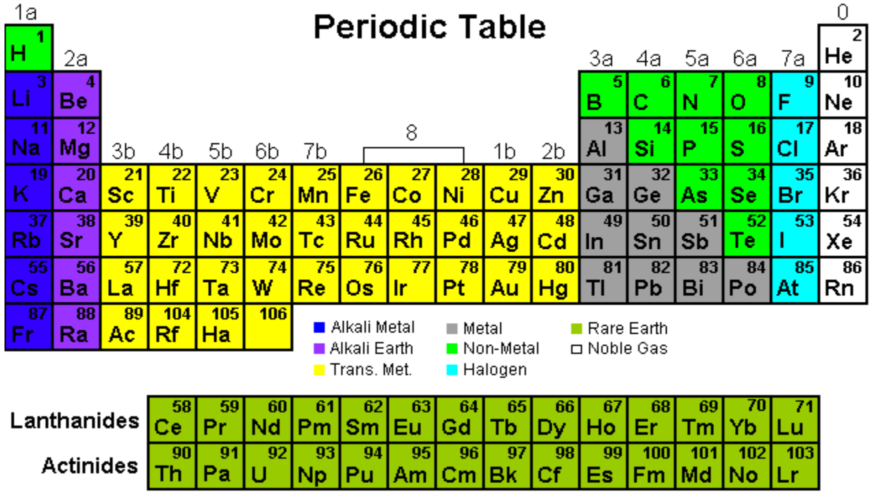

Periodic Table

1a	2a	3b	4b	5b	6b	7b	8			1b	2b	3a	4a	5a	6a	7a	0
1 H																	2 He
3 Li	4 Be											5 B	6 C	7 N	8 O	9 F	10 Ne
11 Na	12 Mg											13 Al	14 Si	15 P	16 S	17 Cl	18 Ar
19 K	20 Ca	21 Sc	22 Ti	23 V	24 Cr	25 Mn	26 Fe	27 Co	28 Ni	29 Cu	30 Zn	31 Ga	32 Ge	33 As	34 Se	35 Br	36 Kr
37 Rb	38 Sr	39 Y	40 Zr	41 Nb	42 Mo	43 Tc	44 Ru	45 Rh	46 Pd	47 Ag	48 Cd	49 In	50 Sn	51 Sb	52 Te	53 I	54 Xe
55 Cs	56 Ba	57 La	72 Hf	73 Ta	74 W	75 Re	76 Os	77 Ir	78 Pt	79 Au	80 Hg	81 Tl	82 Pb	83 Bi	84 Po	85 At	86 Rn
87 Fr	88 Ra	89 Ac	104 Rf	105 Ha	106												

■ Alkali Metal
■ Alkali Earth
■ Trans. Met.
■ Metal
■ Non-Metal
■ Halogen
■ Rare Earth
□ Noble Gas

Lanthanides	58 Ce	59 Pr	60 Nd	61 Pm	62 Sm	63 Eu	64 Gd	65 Tb	66 Dy	67 Ho	68 Er	69 Tm	70 Yb	71 Lu
Actinides	90 Th	91 Pa	92 U	93 Np	94 Pu	95 Am	96 Cm	97 Bk	98 Cf	99 Es	100 Fm	101 Md	102 No	103 Lr

- Crystal and magnetic structure

No experimental data

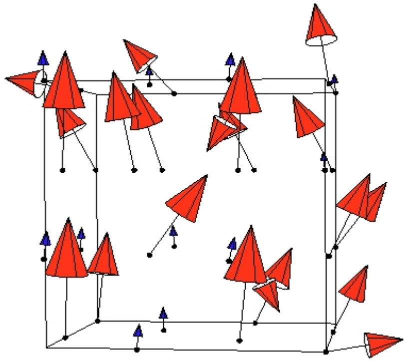

No adjustable parameters

Output from *ab-initio* calculations

- Total energy as a function of ...
  - Volume
  - Crystal structure
  - Distortion
  - Magnetic structure
  - Composition
  - Chemical/magnetic order
  - Defect concentration
  - *etc*.

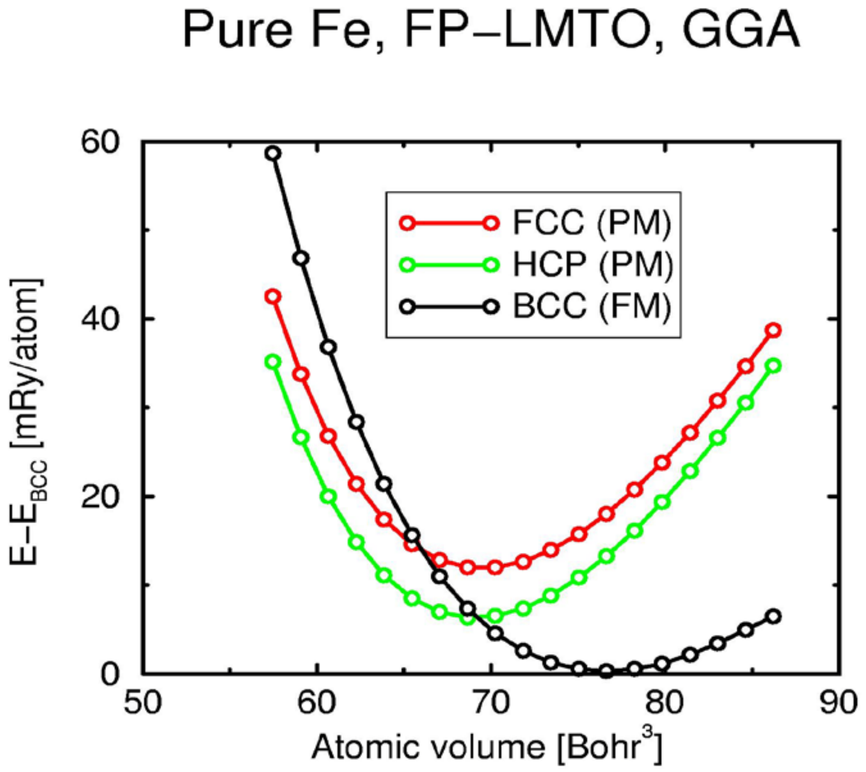

Elastic constants: $C \sim d^2E/d\varepsilon^2$

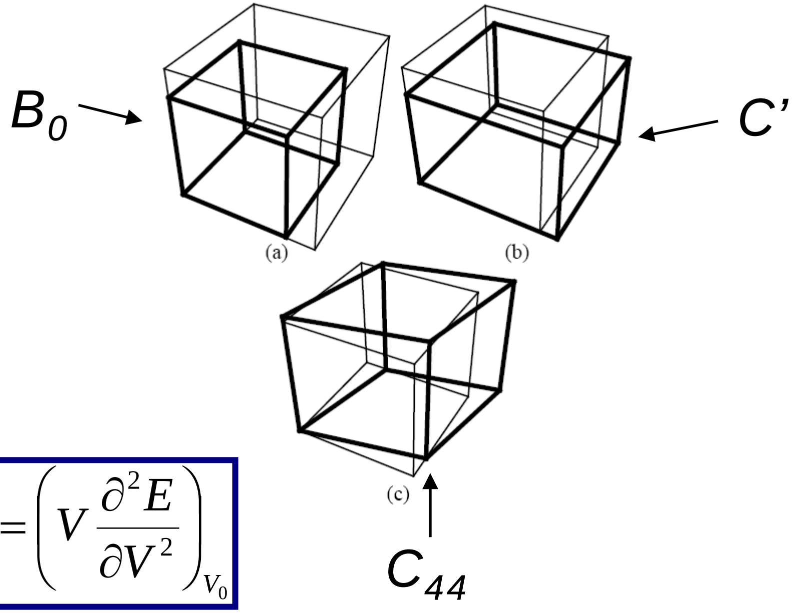

Equilibrium volume, V_0 : $\boxed{\left(\frac{\partial E}{\partial V}\right)_{V_0} = 0 \text{ or } P(V_0) = 0}$

Pressure: $\boxed{P(V) = -\frac{\partial E}{\partial V}}$ Bulk modulus: $\boxed{B_0 = -\left(V\frac{\partial P}{\partial V}\right)_{V_0} = \left(V\frac{\partial^2 E}{\partial V^2}\right)_{V_0}}$

Including atomic motion (molecular dynamics).

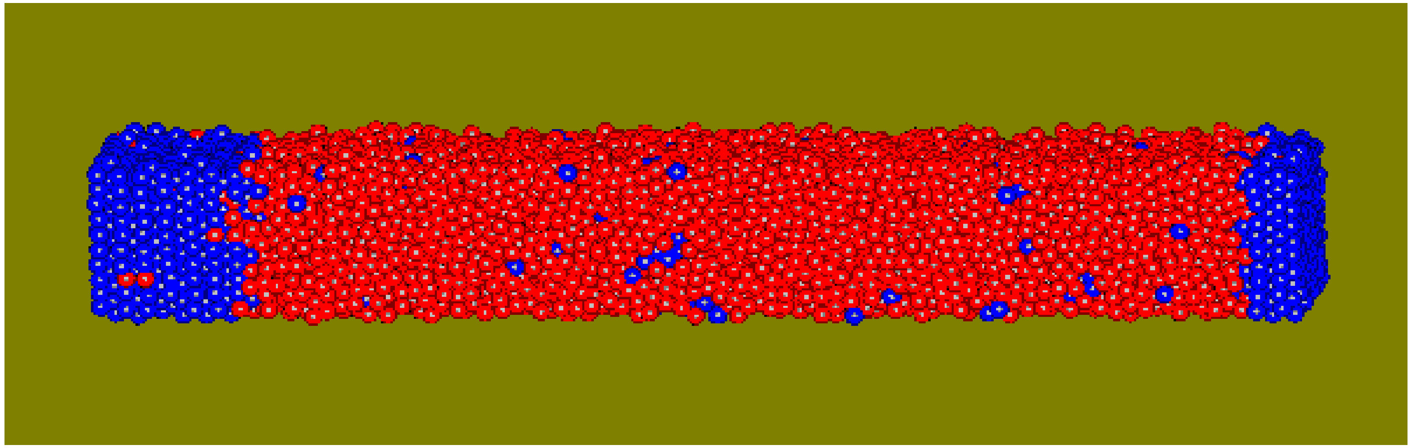

Article: J. J. Hoyt, M. Asta and A. Karma, *Method for Computing the Anisotropy of the Solid-Liquid Interfacial Free Energy,* Phys. Rev. Lett. **86**, 5530-5533 (2001). **See also:** http://cms.northwestern.edu/Intro.html

Potential energy for a system of N particles

$$U = U(\mathbf{r}_1, \mathbf{r}_2, \ldots, \mathbf{r}_N) = U_0 + \sum_i U(\mathbf{r}_i)$$

$$+ \frac{1}{2} \sum_{i,j} V^{(2)}(\mathbf{r}_i, \mathbf{r}_j) + \frac{1}{6} \sum_{i,j,k} V^{(3)}(\mathbf{r}_i, \mathbf{r}_j, \mathbf{r}_k) + \ldots$$

(pair potential) **(3-body potential)**

$$+ \frac{1}{N!} \sum_{i,j,\ldots,n} V^{(N)}(\mathbf{r}_i, \mathbf{r}_j, \ldots, \mathbf{r}_n)$$

(N-body potential)

Atomic motion: Phonons.

Hamiltonian for atomic motion (harmonic approx.)

$$H = \frac{1}{2}\sum_i M_i[\dot{u}(i)]^2 + \frac{1}{2}\sum_{i,j} u^T(i)\Phi(i,j)u(j),$$

Theory: X.Dai *et al.*, *Science* **300**, 953 (2003).
Expt: J. Wong *et al.*, *Science* **301** 1078 (2003).

Force constants

$$\Phi_{\alpha\beta}(i,j) = \left.\frac{\partial^2 E}{\partial u_\alpha(i)\,\partial u_\beta(j)}\right|_{u(l)=0\forall l}$$

Dynamical matrix to diagonalize

$$D = \begin{pmatrix} \frac{\Phi(1,1)}{\sqrt{M_1 M_1}} & \cdots & \frac{\Phi(1,N)}{\sqrt{M_1 M_N}} \\ \vdots & \ddots & \vdots \\ \frac{\Phi(N,1)}{\sqrt{M_N M_1}} & \cdots & \frac{\Phi(N,N)}{\sqrt{M_N M_N}} \end{pmatrix}$$

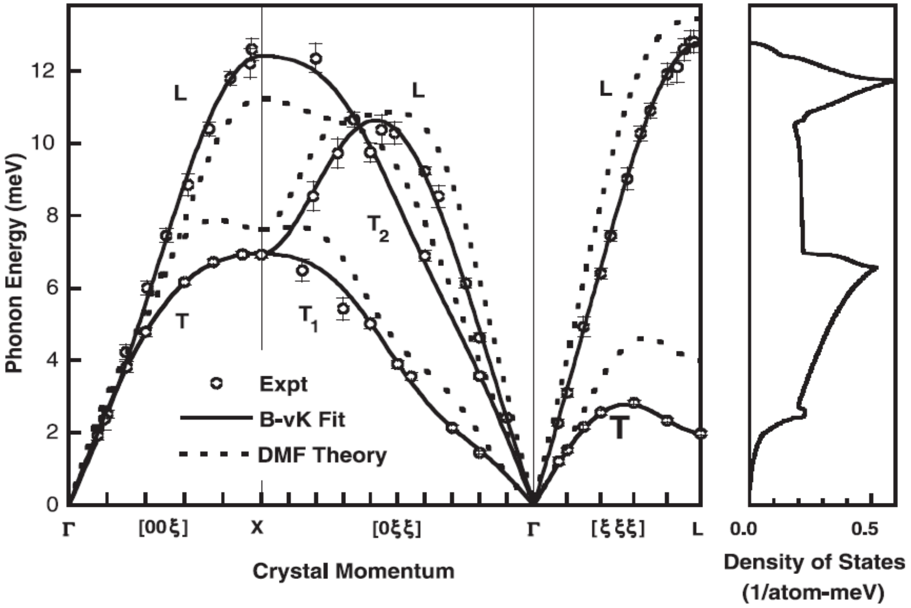

Fig. 2. Phonon dispersions along high-symmetry directions in δ-Pu–0.6 weight % Ga alloy. The longitudinal and transverse modes are denoted L and T, respectively. The experimental data are shown as circles. Along the [0ξξ] direction, there are two transverse branches, [011]⟨011⟩ (T_1) and [011]⟨100⟩ (T_2). The softening of the TA[111] branch toward the L point is apparent. The lattice parameter of our samples is a = 0.4621 nm. The solid curves are the fourth-nearest neighbor Born–von Kármán (B-vK) model fit. The derived phonon density of states, normalized to three states per atom, is plotted in the right panel. The dashed curves are calculated dispersions for pure δ-Pu based on DMFT (*6*).

See A. van de Walle and G. Ceder, *RMP* **74**, 11 (2002) for a review.

Phonon spectrum of Cu_2O

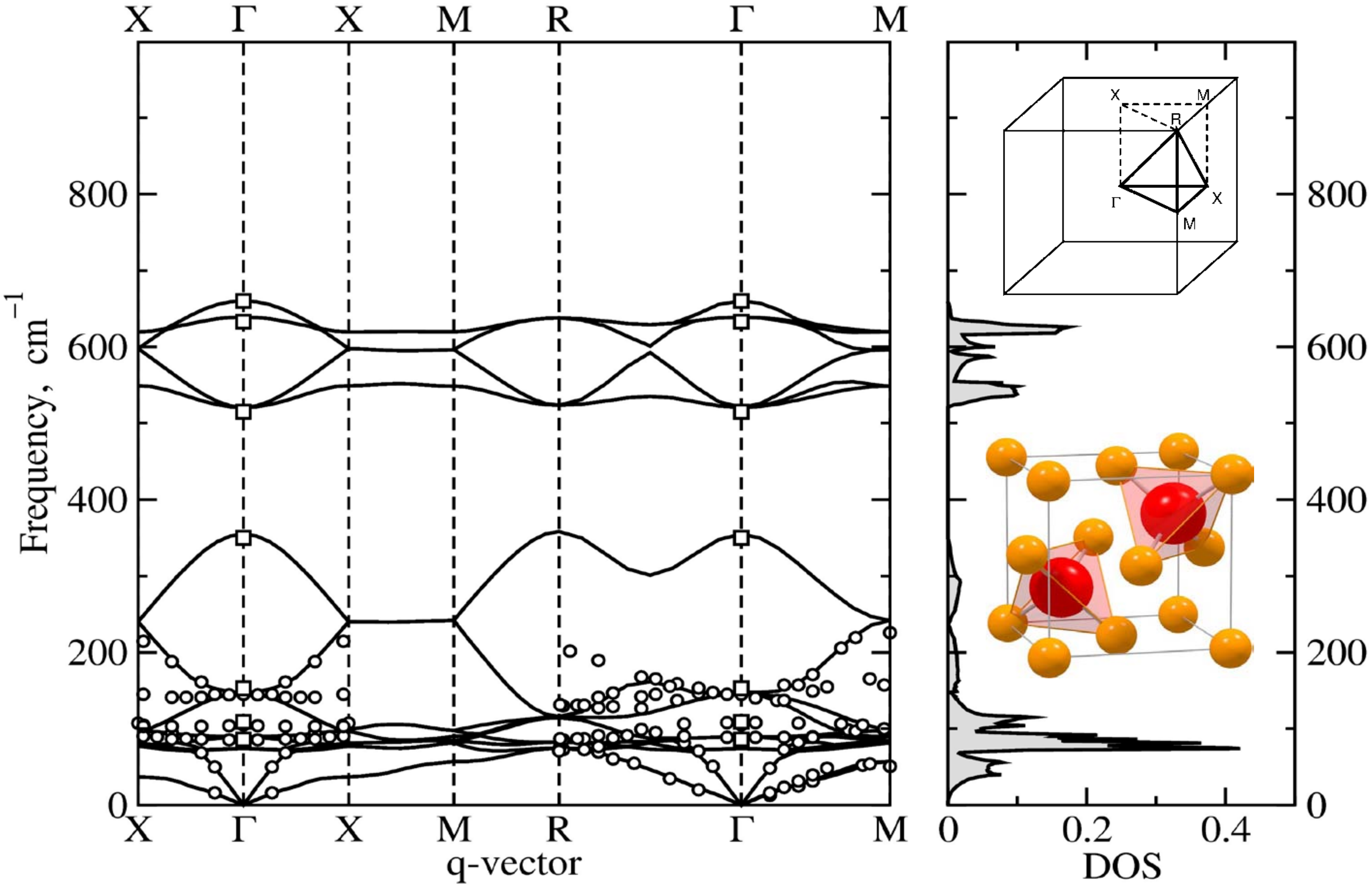

P.A. Korzhavyi and B. Johansson, Technical Report TR-10-30, (SKB, Stockholm, 2010).

Thermodynamic properties of Cu_2O

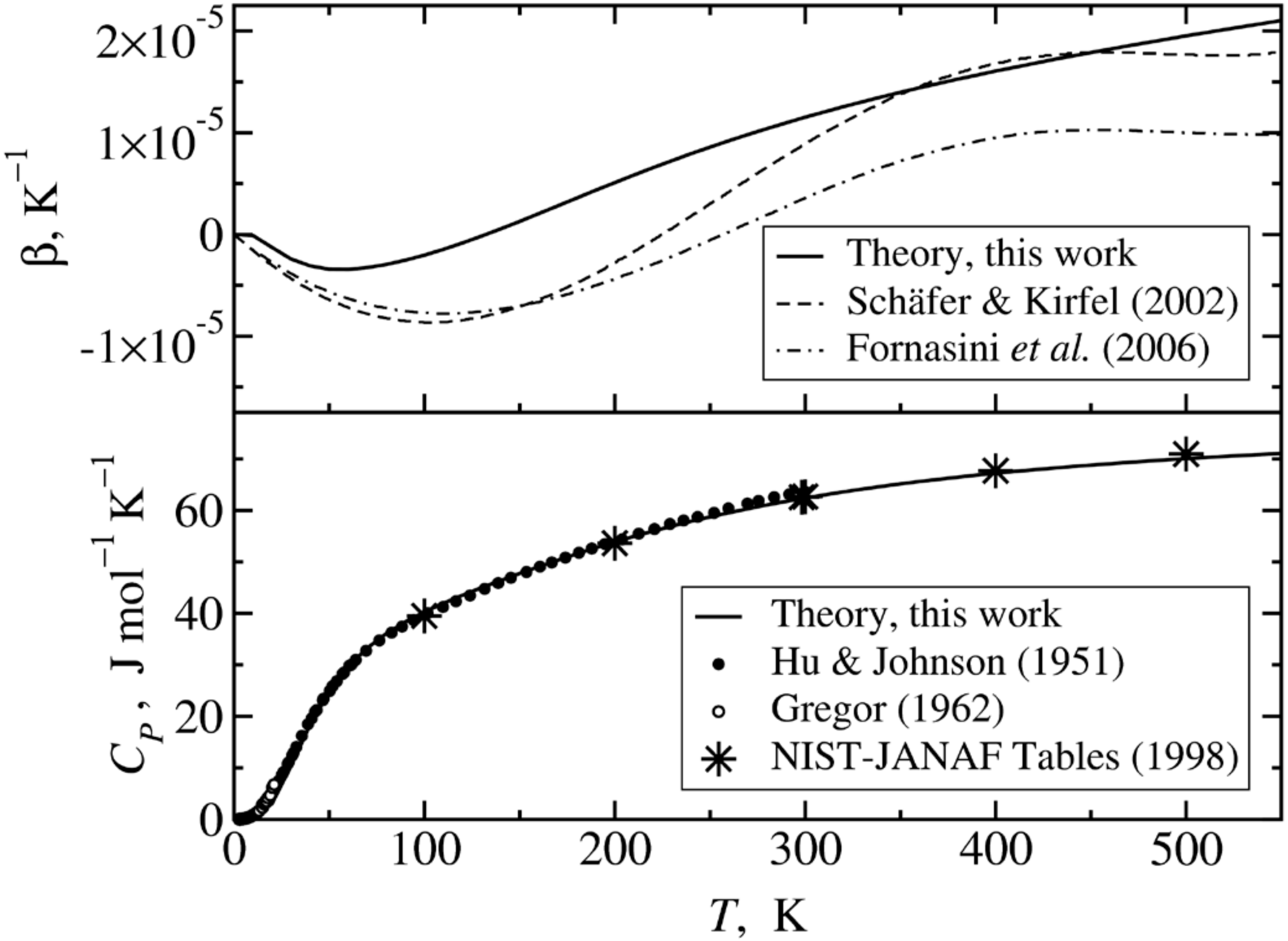

Volume coefficient of thermal expansion

Heat capacity

$$E_0 = U_0 + \frac{1}{2}\int_0^\infty \hbar\omega g(\omega)d\omega$$

$$C_V = k_B \int_0^\infty \left(\frac{\hbar\omega}{2k_B T}\right)^2 \frac{g(\omega)d\omega}{\sinh^2(\hbar\omega/2k_B T)}$$

$$E(T) = E_0 + \int_0^\infty \frac{\hbar\omega g(\omega)d\omega}{\exp\,(\hbar\omega/k_B T) - 1}$$

$$F(T) = U_0 + k_B T \int_0^\infty \log\left[2\sinh\left(\hbar\omega/\ 2k_B T\right)\right]d\omega$$

Bonding in simple metals

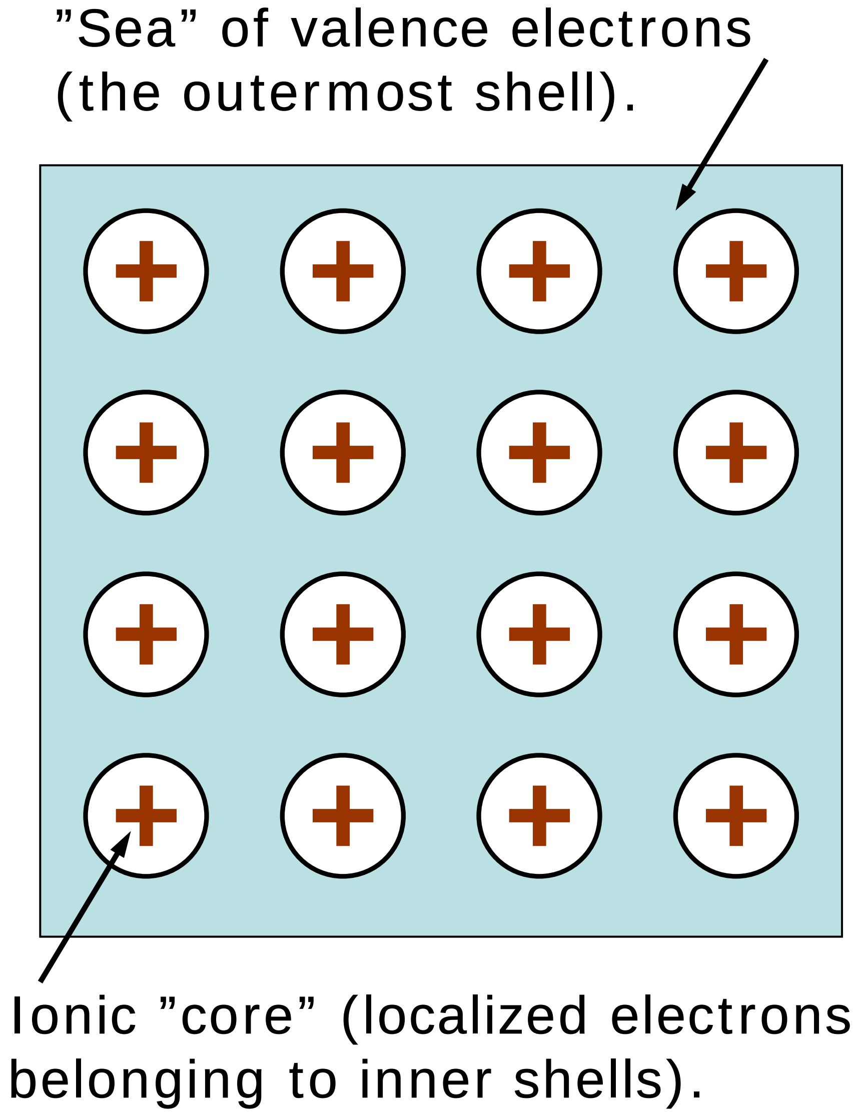

”Sea” of valence electrons (the outermost shell).

Ionic ”core” (localized electrons belonging to inner shells).

Pair potential between two ions in a simple metal is the result of a direct Coulomb interaction between ions and of an ***indirect*** interaction due to scattering of valence electrons on ions.

The ***indirect*** interaction is a purely quantum-mechanical effect. Many ions can participate in the interaction process. This leads, in general, to multi-atom (many-body) interactions.

Thermodynamics and magnetism of iron

PHYSICAL REVIEW VOLUME 102, NUMBER 6 JUNE 15, 1956

Components of the Thermodynamic Functions of Iron

R. J. WEISS AND K. J. TAUER*
Ordnance Materials Research Office, Watertown Arsenal, Watertown, Massachusetts
(Received January 23, 1956)

Hillert & Jarl (1978)

Magnetic energy, α-Fe:

$$E_{\text{magn}} = \int_{0}^{\infty} C_{\text{magn}}\, dT \quad \cong \mathbf{1103\ K}$$

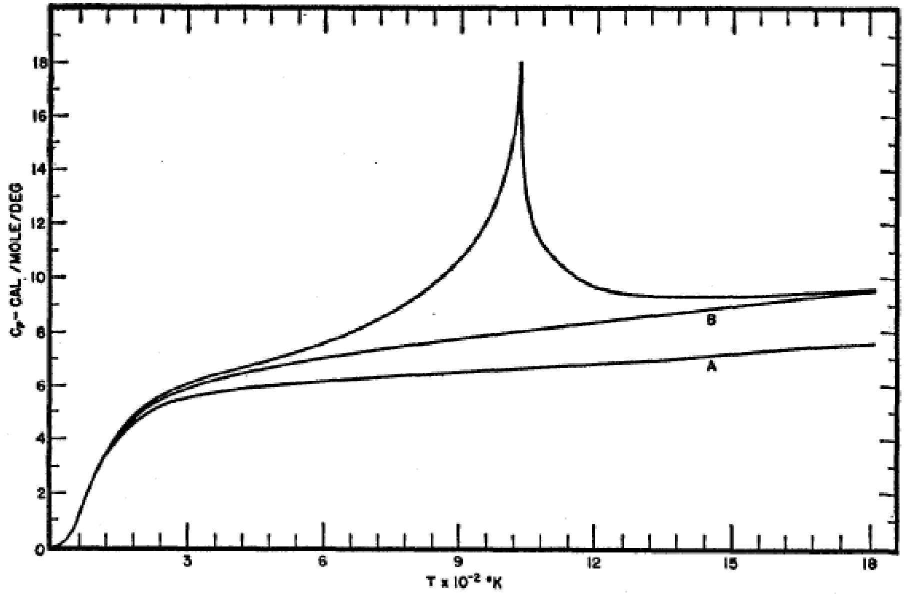

FIG. 1. Specific heat of α (b.c.c.) Fe. Curve *A* is the calculated lattice specific heat for a Debye θ=420°K. Curve *B* includes the electronic specific heat.

Magnetic entropy , α-Fe:

$$S_{\text{magn}} = \int_{0}^{\infty} \frac{C_{\text{magn}}}{\mathrm{T}}\, dT \cong R\ln(2s+1) \cong \mathbf{1.169 \cdot \mathit{R}}$$

First-principles approach to iron and steel

Levente Vitos

Hans Skriver

Andrei Ruban

Igor Abrikosov

Pure Fe: EMTO, GGA

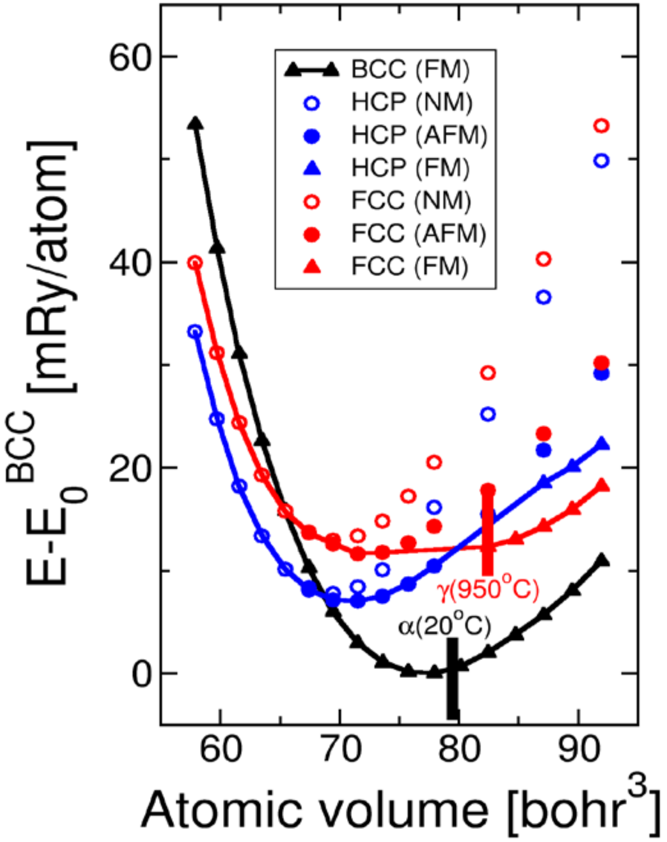

Exact Muffin-Tin Orbitals theory

(O.K. Andersen 1994, L. Vitos, H.L. Skriver 2000)

Coherent Potential Approximation

-chemical and magnetic disorder

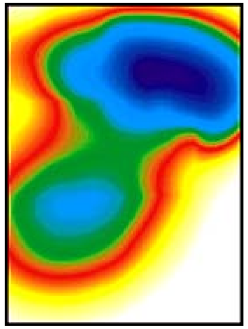

EMTO-CPA method

L. Vitos, I.A. Abrikosov, B. Johansson, Phys. Rev. Lett. **87**, 156401 (2001).

Coherent potential approximation (CPA)

P.Soven, Phys. Rev. **156**, 809 (1967).
D.W.Taylor, Phys. Rev. **156**, 1017 (1967).

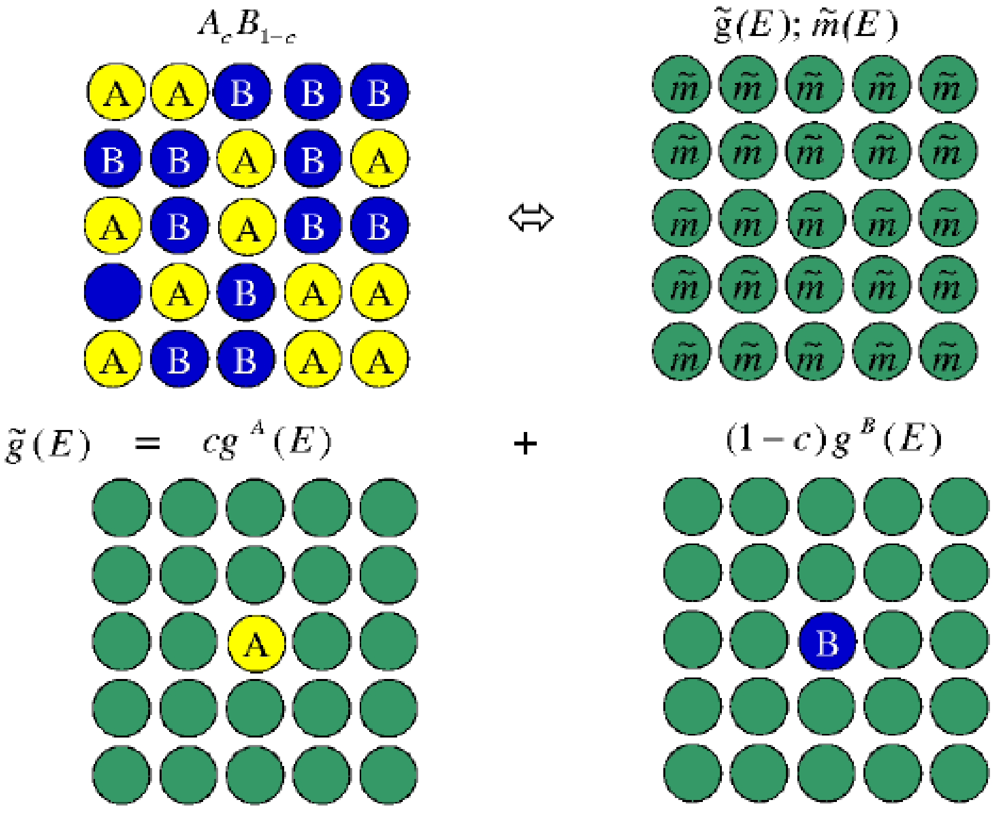

Disordered Local Moment (DLM) model
J. Staunton, B.L. Györffy A.J.Pindor, G.M. Stocks, and H. Winter, JMMM **45**, 15 (1984).

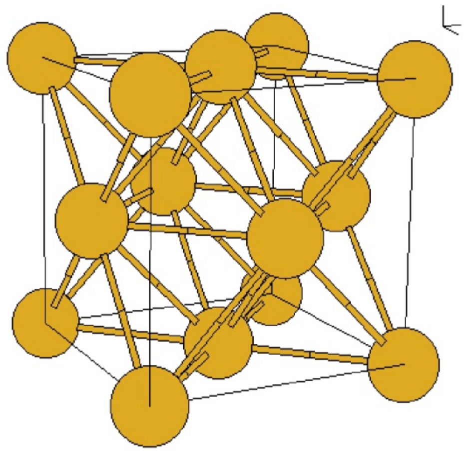

50% Fe↑+ 50% Fe↓

Magnetic entropy:

$$\boxed{S_{magn} = k_B \ln(M_s + 1)}$$

J.S. Faulkner: "*The modern theory of alloys*", Progr. Mater. Science **27**, 1 – 187 (1982).
A.V. Ruban and I.A. Abrikosov: "*Configurational thermodynamics of alloys from first principles: effective cluster interactions*", Rep. Prog. Phys. **71**, 046501 (2008)

Order(N) – Linear Scaling Methods

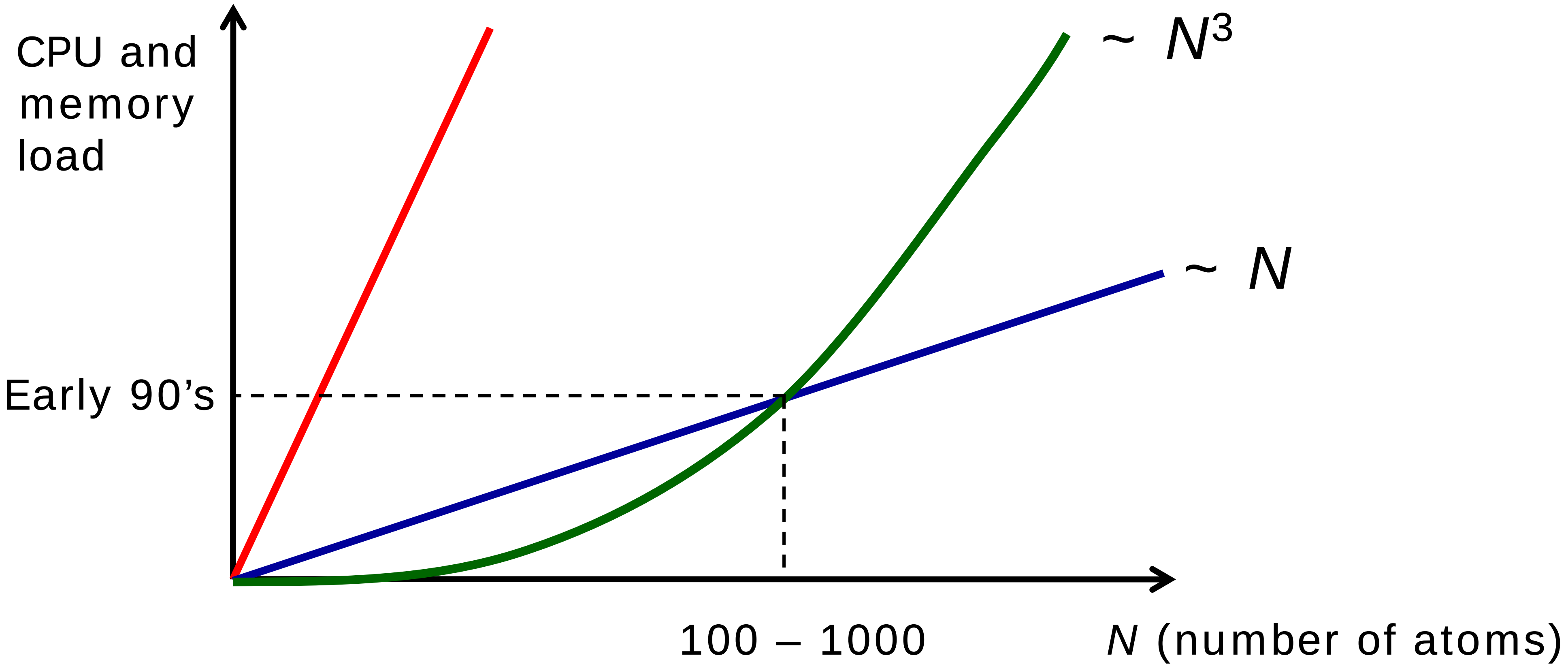

Reviews on $O(N)$ Methods:

S. Goedecker, Rev. Mod. Phys. 71, (1999); http://arXiv.org/abs/cond-m3at/980607.

P. Ordejón, Comp. Mat. Sci. 12, 157 (1998).

Key to linear scaling: locality

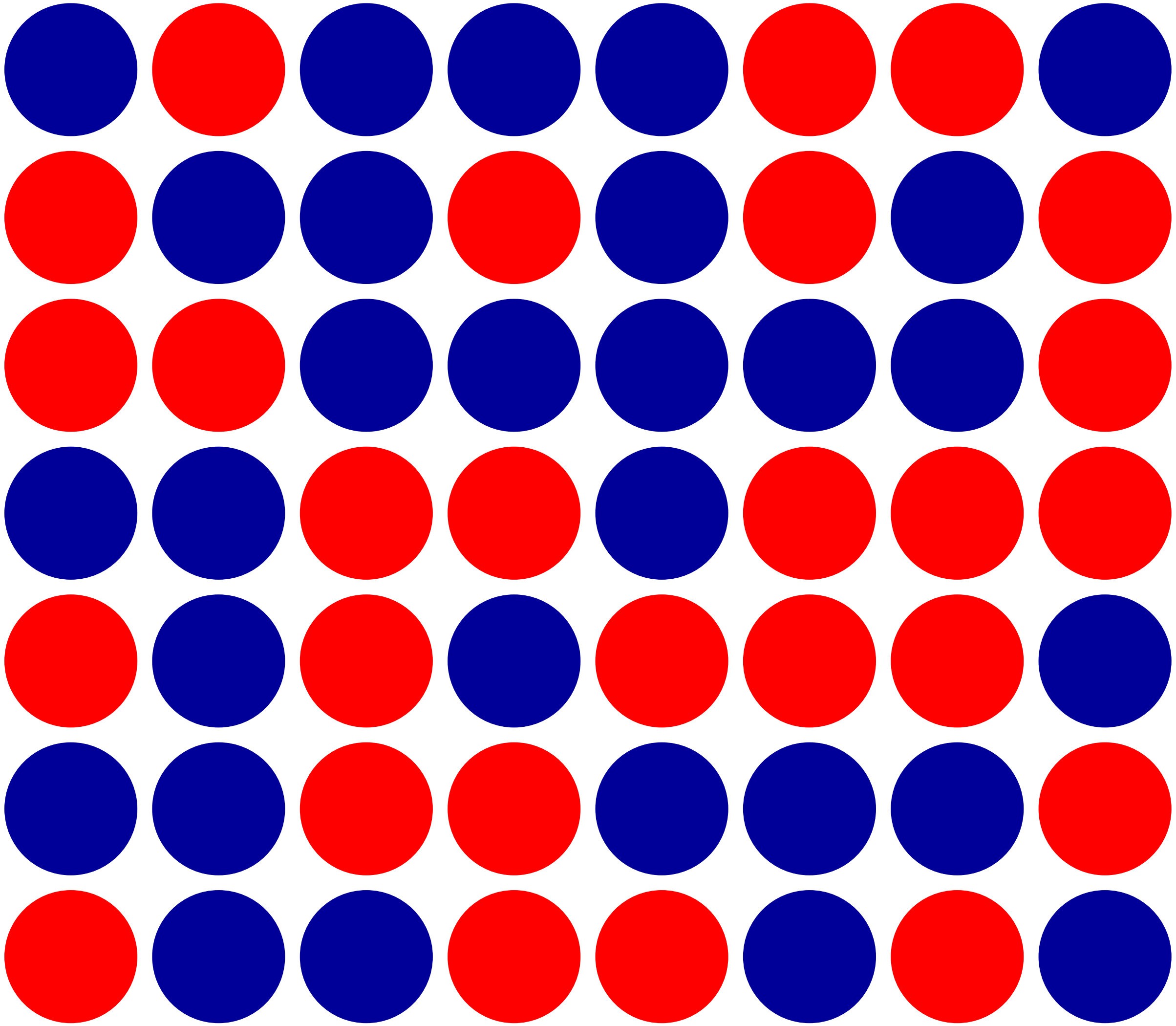

Locally Self-consistent Green’s Function (LSGF) method:

I.A. Abrikosov *et. al.*, , Phys. Rev. Lett. **76**, 4203 (1996);

I.A. Abrikosov *et. al.*, , Phys. Rev. B **56**, 9319 (1997).

Key to linear scaling: locality

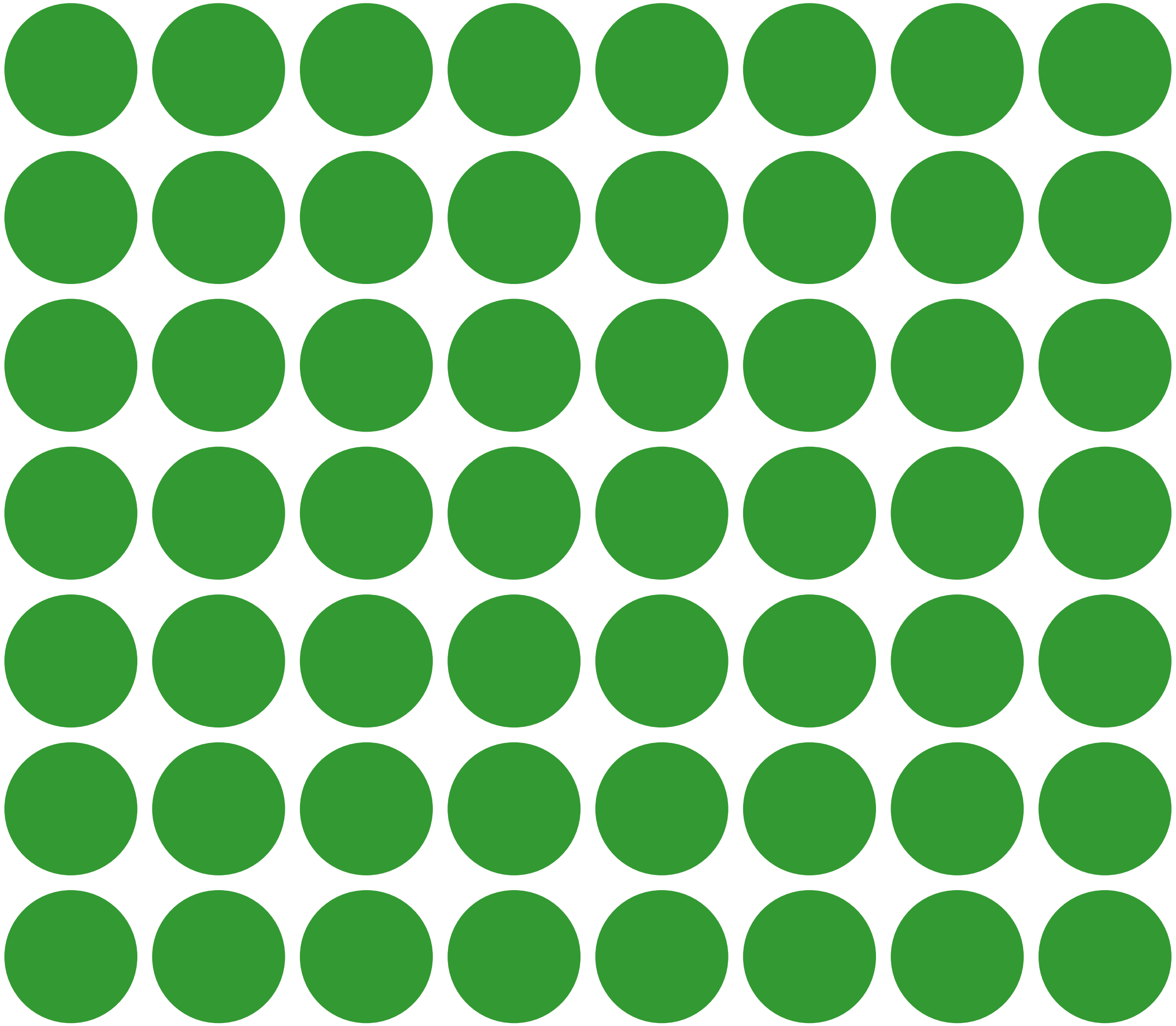

Locally Self-consistent Green's Function (LSGF) method:

I.A. Abrikosov *et. al.*, , Phys. Rev. Lett. **76**, 4203 (1996);

I.A. Abrikosov *et. al.*, , Phys. Rev. B **56**, 9319 (1997).

Key to linear scaling: locality

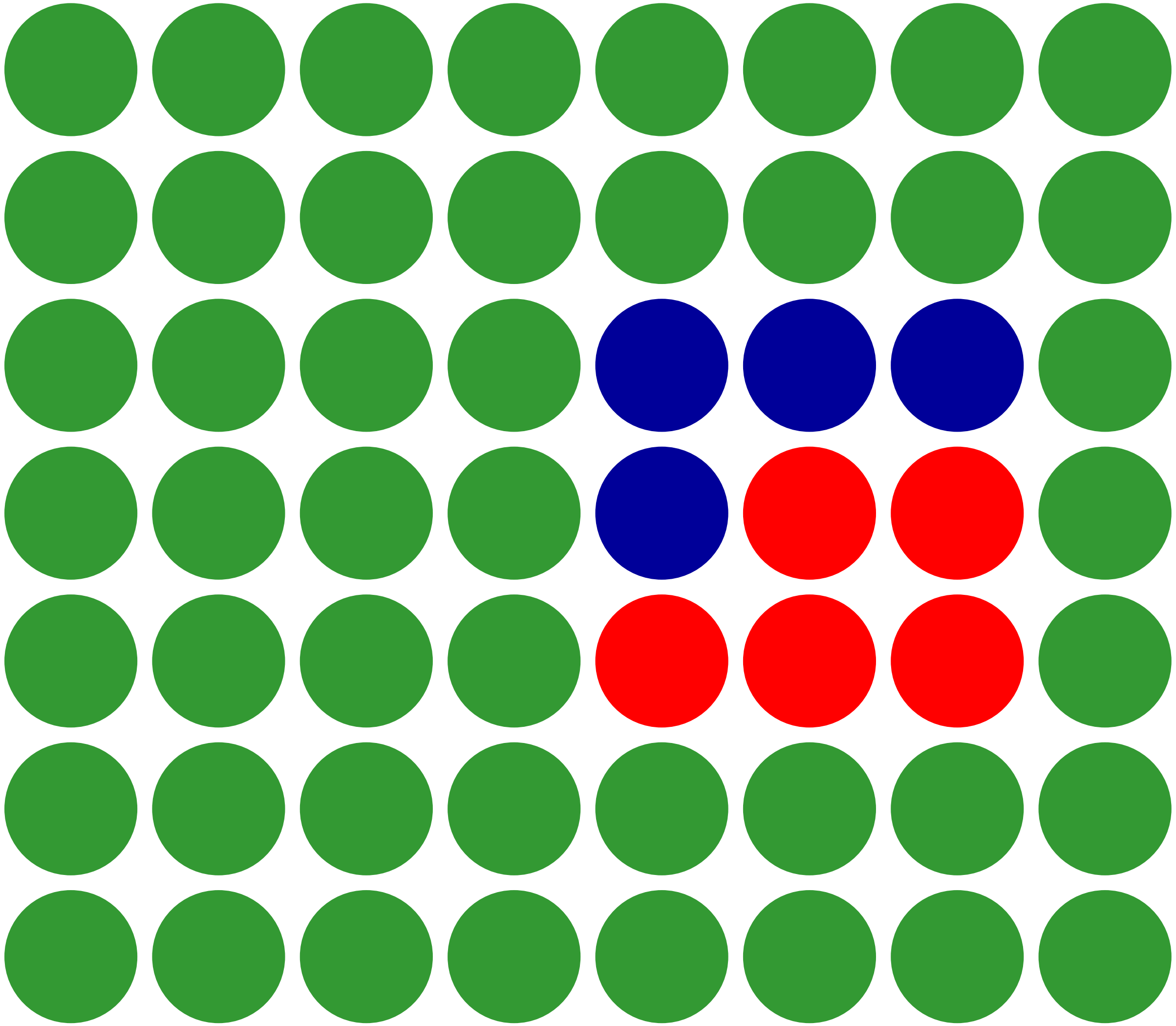

Locally Self-consistent Green's Function (LSGF) method:

I.A. Abrikosov *et. al.*, , Phys. Rev. Lett. **76**, 4203 (1996);

I.A. Abrikosov *et. al.*, , Phys. Rev. B **56**, 9319 (1997).

Key to linear scaling: locality

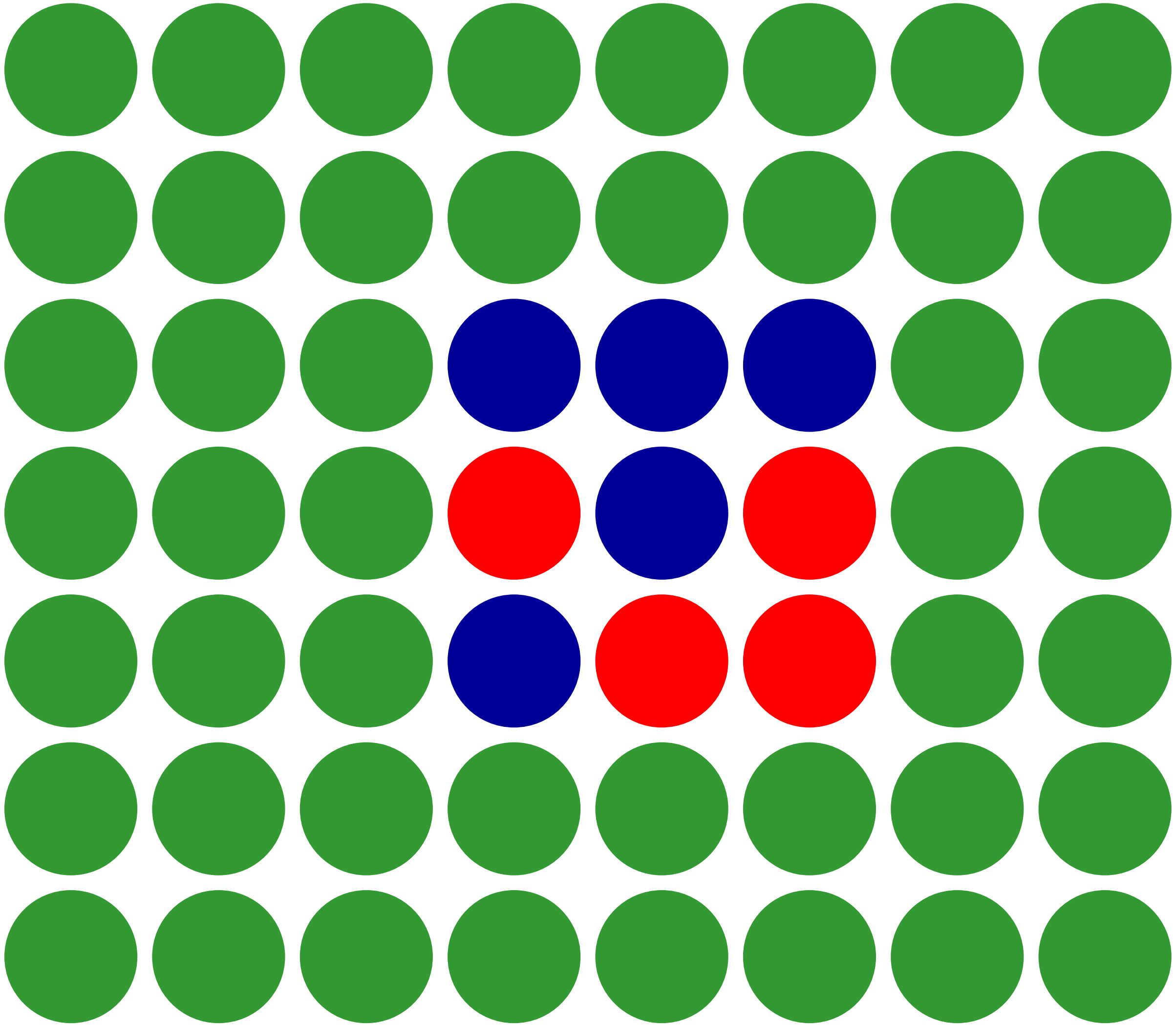

Locally Self-consistent Green's Function (LSGF) method:

I.A. Abrikosov *et. al.*, , Phys. Rev. Lett. **76**, 4203 (1996);

I.A. Abrikosov *et. al.*, , Phys. Rev. B **56**, 9319 (1997).

Linear scaling methods (LSGF, SIESTA): access to large systems (disorder, defects).

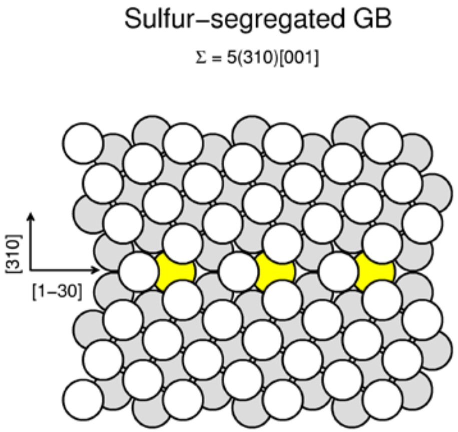

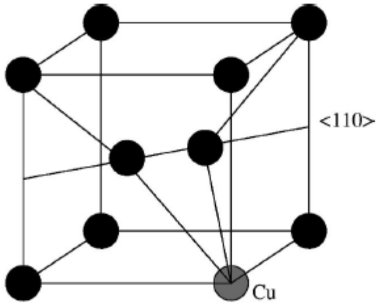

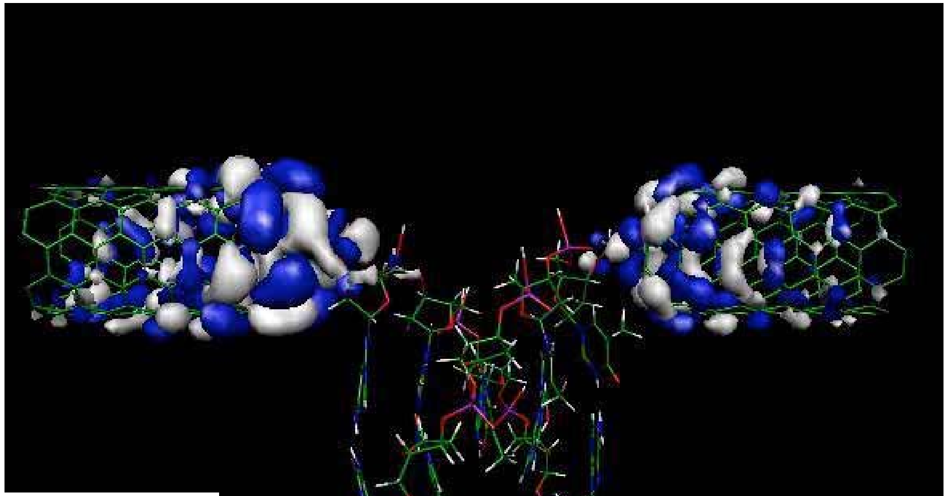

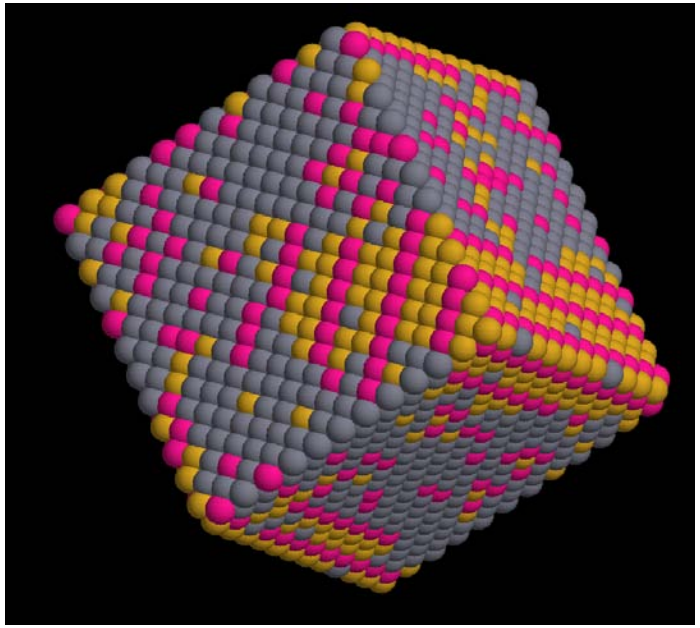

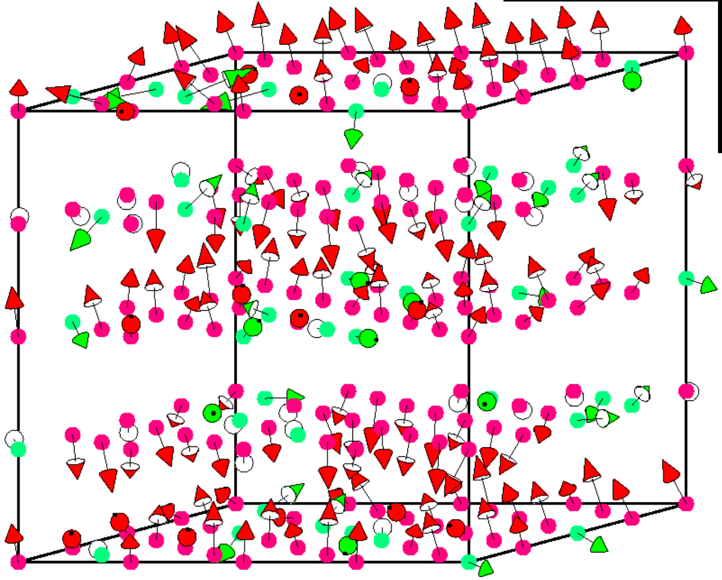

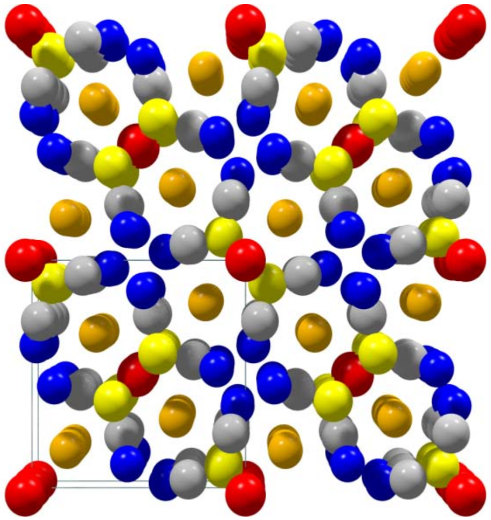

Cu precipitation in Fe: a serious issue for nuclear reactor safety

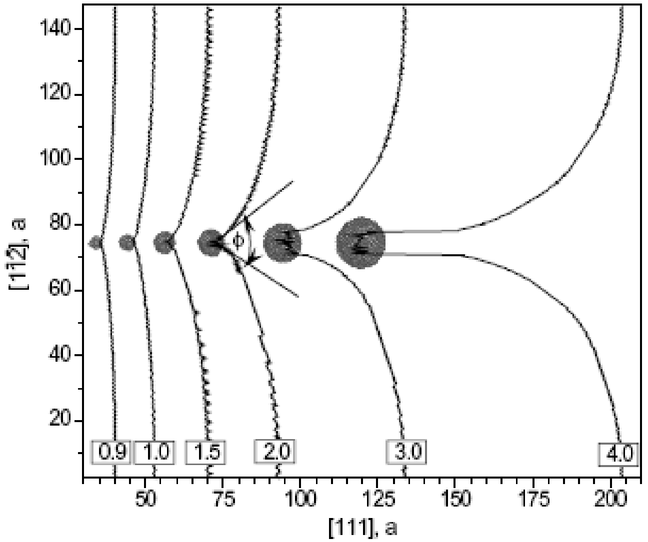

Fig. 2. Dislocation line in the $(1\bar{1}0)$ slip plane at the critical stress τ_c for different precipitate sizes at 0 K.

- Nano-sized precipitates of bcc Cu form under irradiation of reactor pressure vessel (RPV) steels
- Cu particles impede dislocation motion by pinning the dislocation lines – strengthening effect
- Increase in yield strength correlates with the increase of brittle-to-ductile transition temperature – embrittlement

K.C. Russell and L.M. Brown: *A dispersion strengthening model based on differing elastic moduli applied to the iron-copper system*, Acta Metall. 20, 969 – 974 (1972).
D.J. Bacon and Yu.N. Osetsky: *Hardening due to copper precipitates in α-iron studied by atomic-scale modelling*, Journal of Nuclear Materials 329–333, 1233–1237 (2004).
N. Sandberg and P. Korzhavyi: *Theoretical study of irradiation induced hardening and embrittlement in spent nuclear fuel holders, relevant for the Swedish long-term storage*, SKB R-09-15 (2009).

Energies of defect clusters from first-principles calculations

In order to make reliable long-term predictions, a firm knowledge of the driving forces and of the atomic mechanisms for precipitation at low temperatures. The challenging task is to deduce these mechanisms and to compute the relevant energies from first principles.

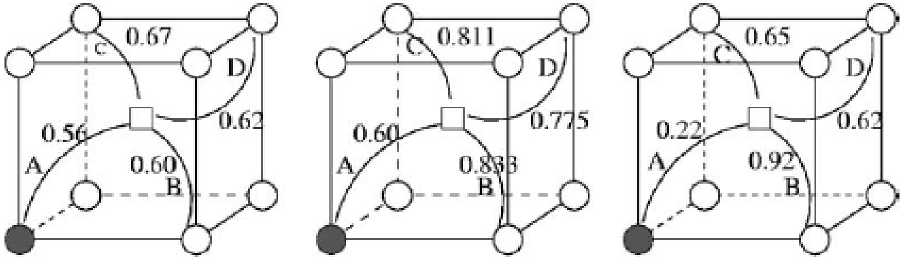

E_{mig}^{Fe} =0.64 eV (a)

E_{mig}^{Fe} =0.77 eV (b)

E_{mig}^{Fe} =0.69 eV (c)

Fig. 2. Vacancy migration energy in a presence of one Cu atom: (a) ab initio, (b) potential FS-1, (c) potential EAM-1. The empty squares are vacancies, the empty circles are Fe atoms and the grey circles are Cu atoms. The bottom caption is the vacancy migration energy in pure Fe.

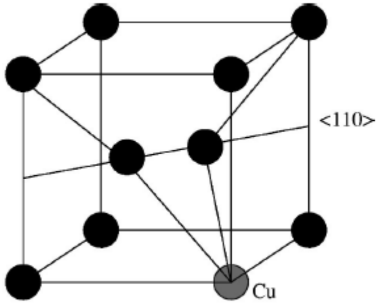

C.S. Becquart and C. Domain: “*Ab initio* contribution to the study of complexes formed during dilute FeCu alloys radiation”, Nuclear Instruments and Methods in Physics Research B, 202, 2003, pp. 44 – 50

Solubility and diffusivity of Cu in Fe from first principles!

F. Soisson and C.-C. Fu: PHYSICAL REVIEW B **76**, 214102 (2007)

CU-PRECIPITATION KINETICS IN α-Fe FROM…

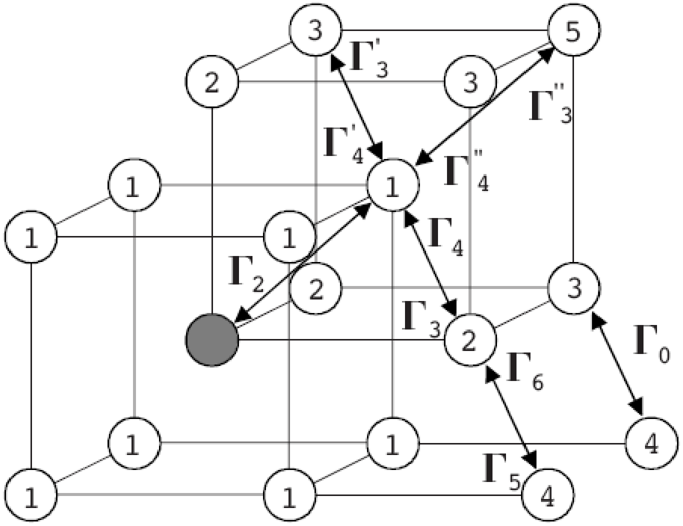

FIG. 2. Vacancy jump frequencies (Γ_i) around a copper atom (gray) and its neighboring iron atoms (white). The arrows indicate the direction of the vacancy jumps; the circled numbers are the order of neighbors to the copper atom.

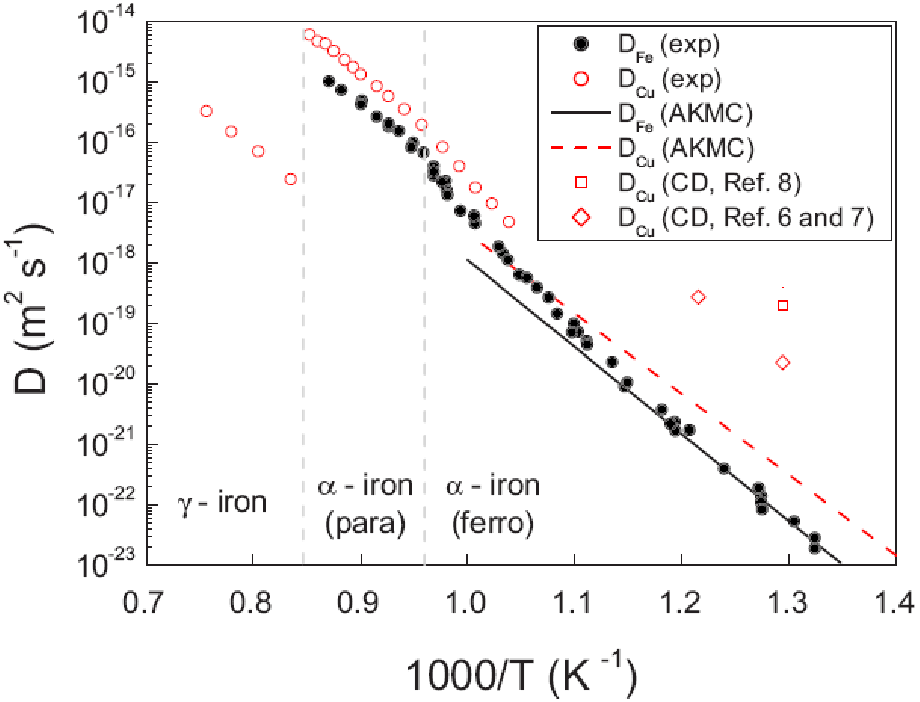

FIG. 5. (Color online) Iron self-diffusion and copper impurity diffusion coefficients. Comparison between the experimental data (Refs. 1 and 36); the coefficients used in our AKMC simulations and the coefficients used in the cluster dynamics modeling of Christien and Barbu (Ref. 8) and Golubov *et al.* (Refs. 6 and 7).

Monte Carlo study of vacancy ordering

Calculated phase diagram

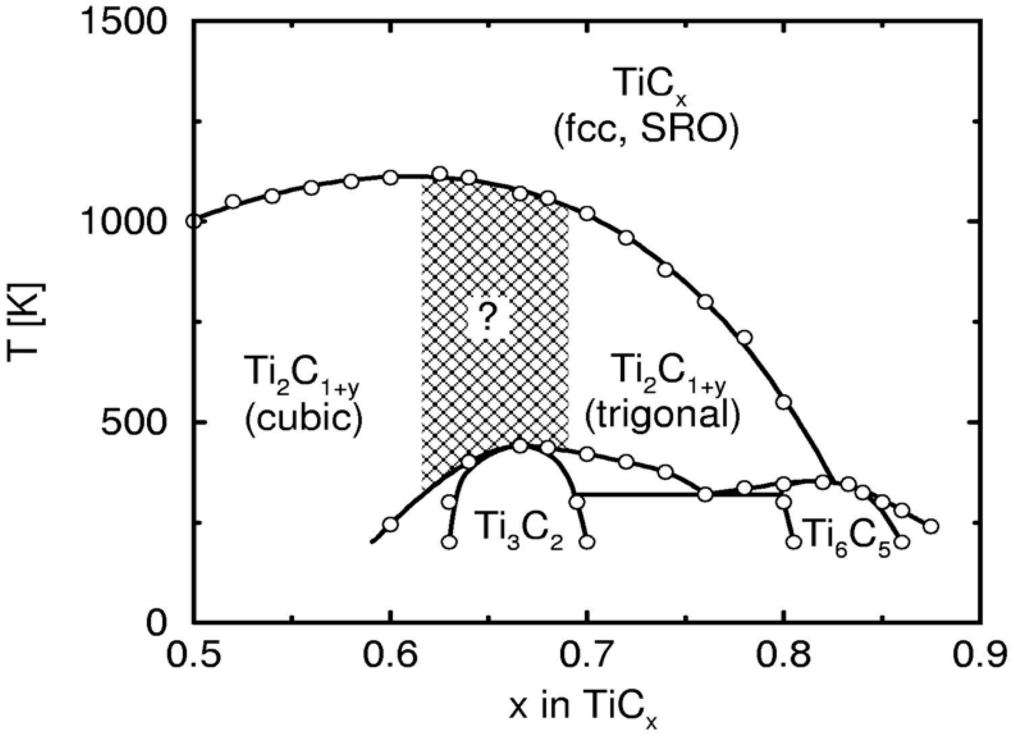

P. Korzhavyi *et al*., Phys. Rev. Lett. 88, 15505 (2002).

Monte Carlo

- Simulation box: 32x32x32 (32768 carbon sites)
- 5000 time steps per site

Order of vacancies in the (111) layers of Ti_3C_2 and Ti_6C_5:

Ordering pattern

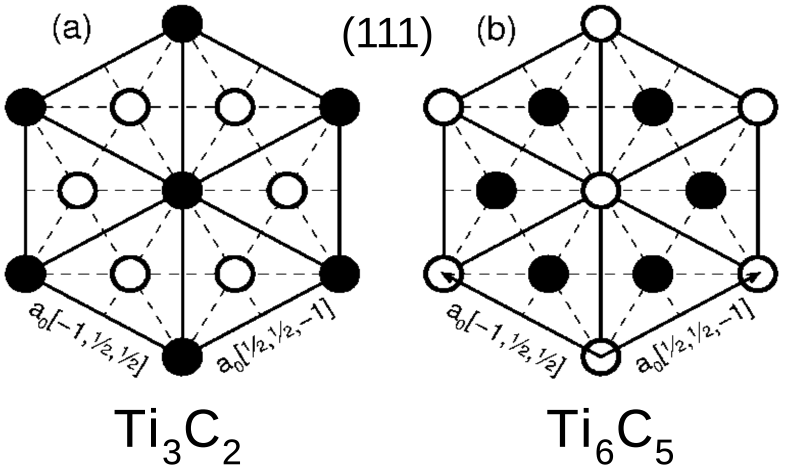

Stacking between layers

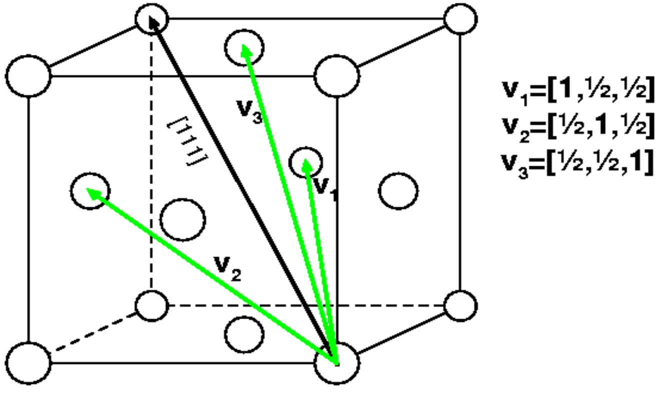

Combined ab initio and Calphad study of vacancy order in $Ti(C,N)_X$

D.A. Andersson, P.A. Korzhavyi and B. Johansson, *"First-principles based calculation of binary and multicomponent phase diagrams for titanium carbonitride"*, CALPHAD, **32**, 543 (2008) **BEST PAPER AWARD (CALPHAD 2009)**

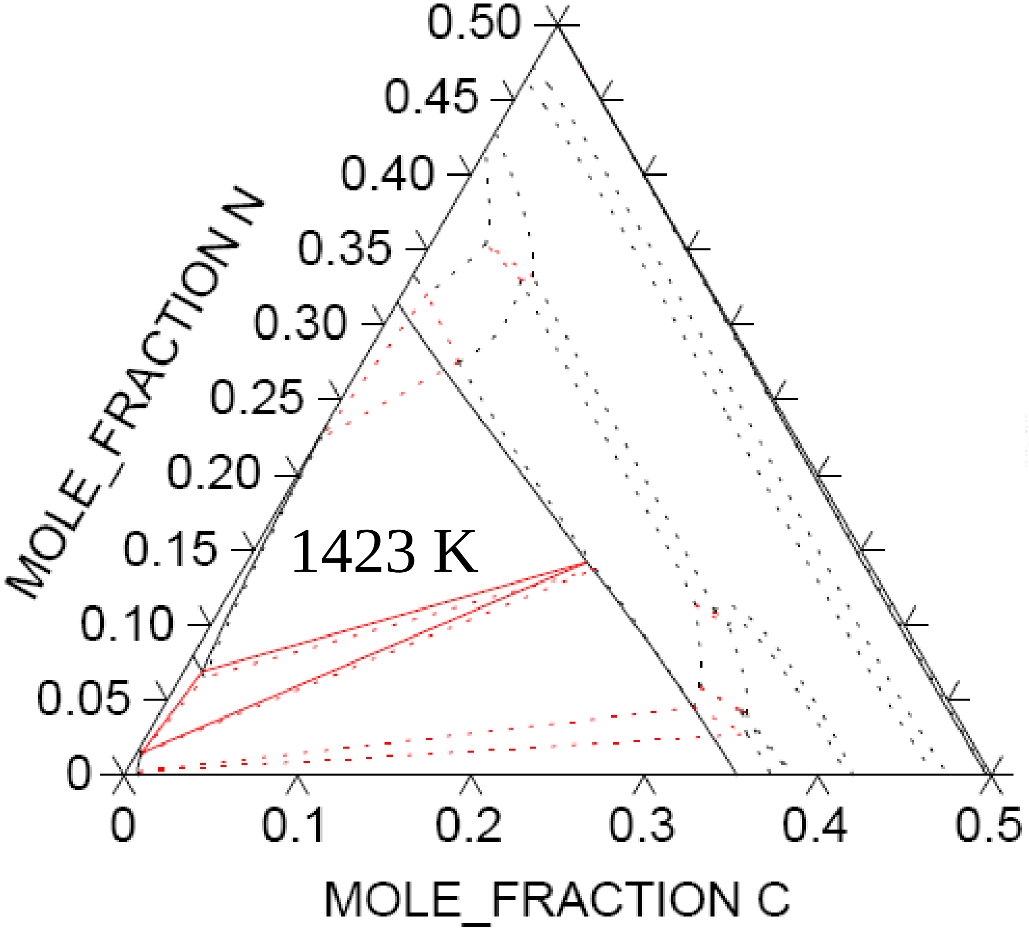

Warren-Cowley SRO at 1423 K

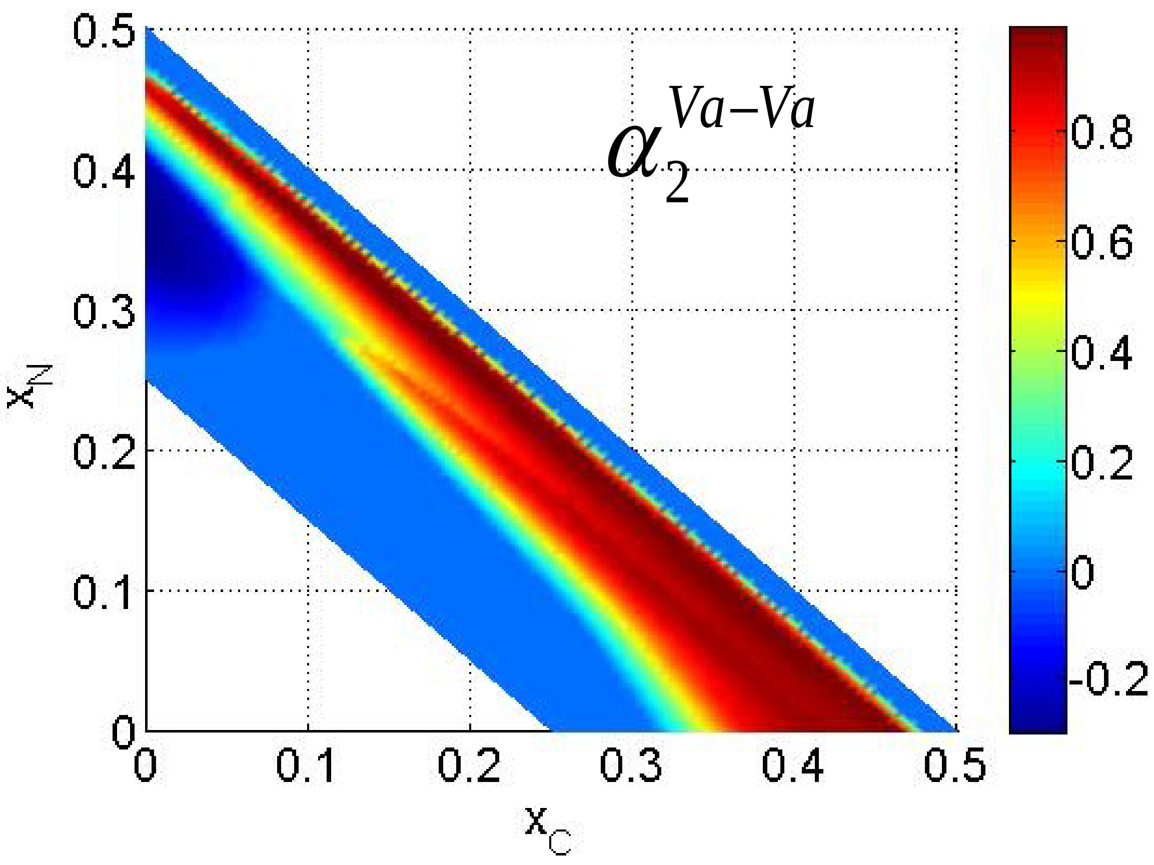

Distinguishing features of *ab-initio* calculations as a modern research tool

- Atomic-scale resolution
- Access to the properties of metastable or unstable systems.
- Access to phase equilibria at low temperatures.
- Excellent control of ”experimental” conditions.
- *Ab intio* calculations are restricted to simple structures, typically <1000 atoms. With $O(N)$ – up to 10^5 atoms.
- In order to access the properties of more realistic (complex) systems, *ab initio* calculations must be combined with statistical-mechanical or thermodynamic modeling (e.g., Molecular Dynamics, Monte Carlo, etc.).